ACS Infectious Diseases

Article

Cite This: ACS Infect. Dis. 2019, 5, 1581−1589

pubs.acs.org/journal/aidcbc

Novel Oleanolic and Maslinic Acid Derivatives as a Promising Treatment against Bacterial Biofilm in Nosocomial Infections: An in Vitro and in Vivo Study

Núria Blanco-Cabra,[†] Karina Vega-Granados,[‡] Laura Moya-Andérico,[†] Marija Vukomanovic,[†] Andrés Parra,[‡] Luis Álvarez de Cienfuegos,*[,‡,§] and Eduard Torrents*[,†]

[†]Bacterial Infections and Antimicrobial Therapies Group, Institute for Bioengineering of Catalonia (IBEC), The Barcelona Institute of Science and Technology (BIST), Baldiri Reixac 15-21, 08028 Barcelona, Spain

[‡]Department of Organic Chemistry, Faculty of Science, University of Granada, Campus Universitario Fuentenueva s/n, 18071 Granada, Spain

[§]Instituto de Investigación Biosanitaria ibs.GRANADA, Universidad de Granada, 18012 Granada, Spain

Supporting Information

ABSTRACT: Oleanolic acid (OA) and maslinic acid (MA) are pentacyclic triterpenic compounds that abound in industrial olive oil waste. These compounds have renowned antimicrobial properties and lack cytotoxicity in eukaryotic cells as well as resistance mechanisms in bacteria. Despite these advantages, their antimicrobial activity has only been tested in vitro, and derivatives improving this activity have not been reported. In this work, a set of 14 OA and MA C-28 amide derivatives have been synthesized. Two of these derivatives, MA-HDA and OA-HDA, increase the in vitro antimicrobial activity of the parent compounds while reducing their toxicity in most of the Gram-positive bacteria tested, including a methicillin-resistant *Staphylococcus aureus*-MRSA. MA-HDA also shows an enhanced in vivo efficacy in a *Galleria mellonella* invertebrate animal model of infection. A preliminary attempt to elucidate their mechanism of action revealed that these compounds are able to penetrate and damage the bacterial cell membrane. More significantly, their capacity to reduce antibiofilm formation in catheters has also been demonstrated in two sets of conditions: a static and a more challenged continuous-flow *S. aureus* biofilm.

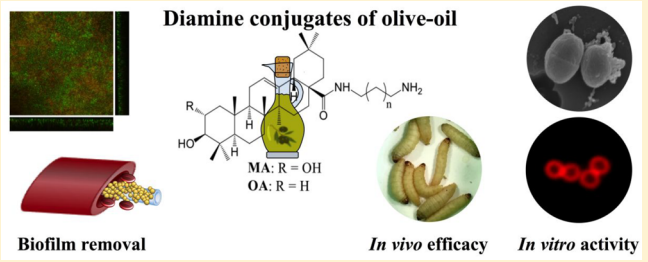

KEYWORDS: *maslinic and oleanolic acids, natural products, in vitro and in vivo antimicrobials, Galleria mellonella, antibiofilm, Staphylococcus aureus*

Staphylococcus aureus is a major global healthcare problem because it is a leading cause of infections in hospitals and the major cause of biofilm formation in catheters and other medical devices like prostheses.[1] Because the bacteria embedded in biofilms can be 100 or even 1000 times more resistant to antibiotics than planktonic-growing bacteria,[2] these *S. aureus* biofilms can generate dangerous infections such as endocarditis, prosthetic joint infection, and even sepsis. The only effective treatment against these biofilms is the removal of the medical device and long-term antibiotic therapy,[3] which can develop antibiotic-resistant bacteria such as methicillin-resistant *S. aureus* (MRSA) and a high increase in the overall treatment cost.[4−6] MRSA infections are more related to bacteremia cases and have poorer clinical outcomes.[4] As a result of the improper use of antibiotics, multiresistant bacteria are a worldwide worrying health problem and cause significant morbidity and mortality. Therefore, there is a critical need to find alternatives to common antibiotics with a smaller risk of resistance development.

Oleanolic acid (OA) and maslinic acid (MA) are pentacyclic triterpenic compounds that can be widely isolated from plants. The function of these triterpenes seems to be protection against dehydration and microbes, as has been noticed with an increase in plant infections when the synthesis of these compounds diminishes.[7,8] They are vastly present in the fruits of *Olea europaea* and consequently abound in industrial olive oil waste.[8,9]

OA and MA have been extensively used in ancestral medicine and have, among others, long-recognized anti-inflammatory, anti-hyperlipidemic, antitumor, and hepatoprotective properties in addition to their known antimicrobial activity.[7,8,10−17] Moreover, these triterpenes have no cytotoxicity on eukaryotic cells, and no resistance mechanisms in bacteria have been found yet.[12] Despite the fact that the exact antimicrobial mechanism of these compounds is still unknown,

Received: April 3, 2019
Published: July 3, 2019

DOI: 10.1021/acsinfecdis.9b00125
ACS Infect. Dis. 2019, 5, 1581−1589

Scheme 1. Synthesis of MA and OA Amine Derivatives

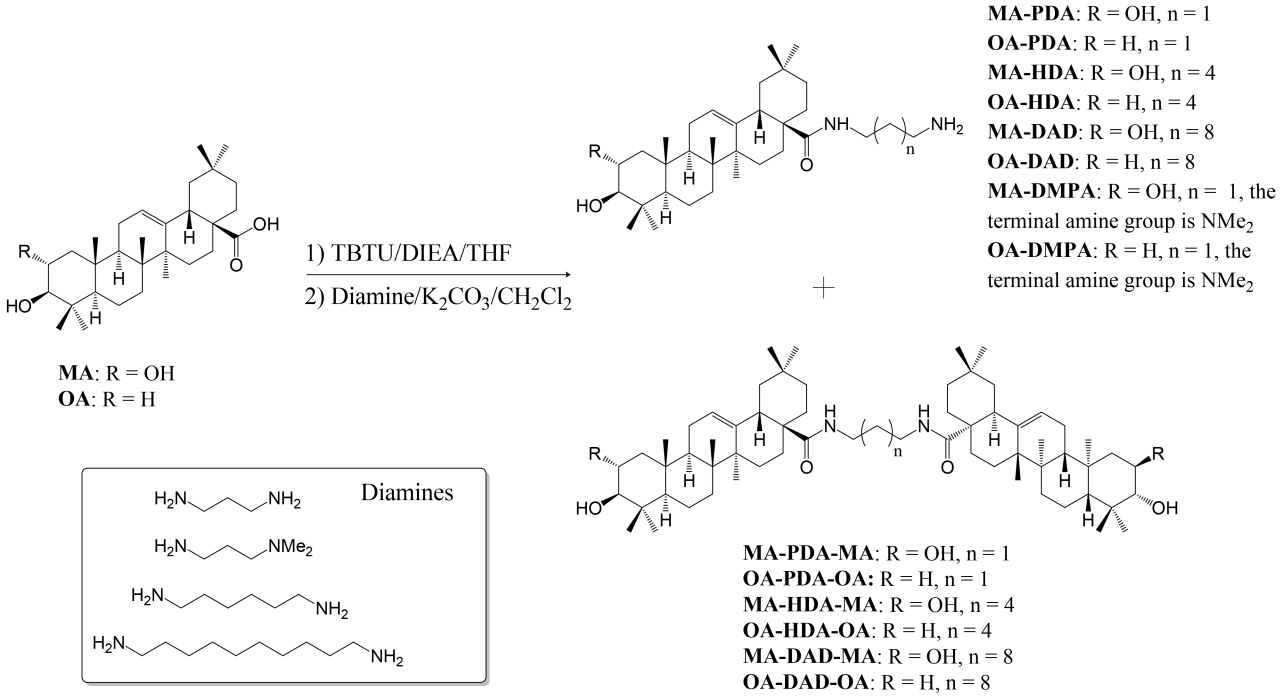

there are some works indicating the peptidoglycan synthesis as the principal target,[10,18] which can explain why these antimicrobial activities have been mostly seen in Gram-positive species, whereas the compounds were devoid of antimicrobial activity against the Gram-negative bacteria tested.[7,10−12,16,17] Despite the antimicrobial activity against Gram-positive bacteria and the lack of toxicity and resistance mechanisms, the activity of OA and MA has only been tested in vitro, and as far as we know, OA and MA derivatives with improved antimicrobial activity are not known.

In this respect, in this work, a set of 14 OA and MA C-28 amide derivatives (Scheme 1 and Table 1) have been synthesized and analyzed for their in vitro and in vivo antimicrobial efficacy and toxicity properties. Moreover, the antibiofilm activity in catheters and flow biofilms of the more active compounds has also been evaluated. The choice of these derivatives was proposed with the aim of simultaneously satisfying two essential criteria. The first one was to obtain two groups of molecules with very different polarities and molecular weights to study which factor could influence the antibacterial activity more. The second one was to obtain these derivatives by means of a simple and direct synthetic strategy which would allow us to obtain, on one hand, derivatives with minimal chemical modifications in order to maintain the low toxicity of the natural OA and MA and, on the other hand, their easy synthesis in large quantities. Furthermore, it has been recently shown that some OA and MA C-28 amide derivatives have enhanced anticancer activity with respect to the natural triterpenes.[13]

For the first time, two of these new derivatives (OA-HDA and MA-HDA) increase the in vitro antimicrobial activity and reduce the toxicity of the parent compounds by reducing the minimum inhibitory concentration (MIC) in most of the Gram-positive bacteria tested, highlighting the efficacy against *S. aureus* and MRSA. Remarkably, MA-HDA also shows enhanced activity in vivo in the *Galleria mellonella* animal model of infection. A preliminary attempt to investigate their mechanism of action shows that these compounds are able to damage the bacterial cell membrane. Their antimicrobial properties have also been evaluated by their antibiofilm capacity. Again, these two derivatives are more effective than their parent compounds in reducing *S. aureus* biofilms in a static and continuous-flow manner. These two derivatives can serve as a guide for the development of useful antimicrobial and antibiofilm agents based on easily accessible natural compounds that can be used alone or in combination with other antimicrobials to promote synergy.[17]

RESULTS AND DISCUSSION

Antibacterial Activity and In Vitro Toxicity. The amide derivatives of oleanolic acid (OA) and maslinic acid (MA) were tested for their antibacterial activity in planktonic bacterial growth. The antibacterial activity that can be seen in Table 1 is represented regarding minimal inhibitory concentration 50% (MIC_{50}) and defined as the compound concentration that inhibits bacterial growth by 50%.

As previously described,[7,10−12,16,17,19] OA and MA inhibited the Gram-positive bacterial growth, whereas no effect was detected against Gram-negative pathogens. Similarly, the amide derivatives tested in this work did not show antibacterial activity against any Gram-negative pathogen tested (Table 1). Cholesterol (C) was used as a negative control. No antimicrobial activity was detected when OA-PDA, OA-DMPA, MA-PDA-MA, OA-PDA-OA, and OA-DAD-OA were used. Furthermore, the diamine chemical precursors HDA and DAD alone did not exhibit any antimicrobial activity at the highest concentration tested (120 μg/mL, data not shown).

Among the 14 derivatives tested in this work, MA-HDA and OA-HDA showed the highest efficacy by maintaining or enhancing the antimicrobial activity of MA and OA in most of the strains tested with particular relevance against *S. aureus* and

DOI: 10.1021/acsinfecdis.9b00125
ACS Infect. Dis. 2019, 5, 1581−1589

Table 1. MIC_{50}, Cytotoxicity, and Selectivity Index (SI) of Compounds[a]

Compound	Formula	MIC_{50} (μg/ml)							CC_{50} (μg/ml)	LD_{50} (mg/kg)
		Gram-Positive					Gram-Negative			
		S. aureus	*S. aureus*-MRSA	*S. epidermidis*	*S. mutans*	*E. faecalis*	*E. coli*	*P. aeruginosa*		
C	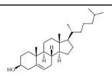	NA	NA	NA	NA	NA	NA	NA	NT	>400
MA	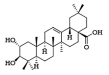	**15 (20.9/504)**	75	**25 (12.5/302)**	**15 (20.9/504)**	**15 (20.9/504)**	NA	NA	314 ± 6	302.44 ± 67
OA	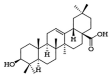	**30 (10.5/302)**	75	200	**30 (10.5/302)**	**30 (10.5/302)**	NA	NA	314 ± 9.8	361.8 ± 70
MA-PDA	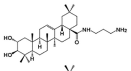	200	200	NA	NA	NA	NA	200	310 ± 5.4	
OA-PDA	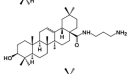	NA	NA	NA	NA	NA	NA	NA	312 ± 8.6	
MA-HDA	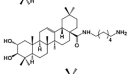	**15 (17.9/661)**	**25 (10.7/397)**	**20 (13.4/496)**	**50 (5.4/198)**	75	NA	NA	268 ± 5.3	396.56 ± 81.2
OA-HDA	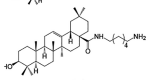	**4 (62.2/1313)**	**10 (24.9/525)**	**5 (49.8/1050)**	**5 (49.8/1050)**	**15 (16.6/350)**	NA	NA	249 ± 10.1	210.08 ± 69.9
MA-DAD	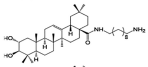	**20 (10.5)**	**25 (8.4)**	**10 (21)**	**25 (8.4)**	**25 (8.4)**	NA	NA	250 ± 10.9	
OA-DAD	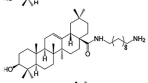	**30 (10.4)**	**30 (10.4)**	**7.5 (41.7)**	**25 (12.5)**	**25 (12.52)**	NA	NA	313 ± 5.3	
MA-DMPA	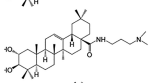	75	85	75	85	75	NA	NA	NT	
OA-DMPA	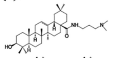	NA	NA	NA	NA	NA	NA	NA	NT	
MA-PDA-MA	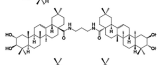	NA	NA	NA	NA	NA	NA	NA	120 ± 19.5	
OA-PDA-OA	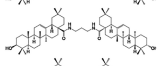	NA	NA	NA	NA	NA	NA	200	NT	
MA-HDA-MA	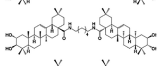	NA	NA	100	100	NA	NA	NA	312 ± 9.4	
OA-HDA-OA	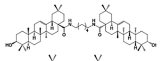	NA	NA	75	100	100	NA	NA	314 ± 12.8	
MA-DAD-MA	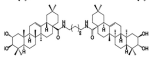	NA	NA	50	NA	NA	NA	NA	317.5 ± 2.9	
OA-DAD-OA	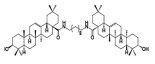	NA	NA	NA	NA	NA	NA	NA	912 ± 3.3	

[a]MIC_{50} was evaluated on: *S. aureus*, *Staphylococcus aureus*; *S. aureus*-MRSA, *Staphylococcus aureus* methicillin-resistant; *S. epidermidis*, *Staphylococcus epidermidis*; *S. mutans*, *Streptococcus mutans*; *E. faecalis*, *Enterococcus faecalis*; *E. coli*, *Escherichia coli*; *P. aeruginosa*, *Pseudomonas aeruginosa*; C, cholesterol. NA, no-activity or MIC_{50} > 250 μg/mL. Cytotoxicity (CC_{50}) was evaluated on human alveolar epithelial A459 cells. NT, non-cytotoxic or CC_{50} > 1000 μg/mL. Lethal doses (LD_{50}) were evaluated in *Galleria mellonella* larvae. Selectivity index (SI), calculated as CC_{50}/MIC_{50} and LD_{50}/MIC_{50}, are indicated in parentheses next to the MIC value.

Methicillin-Resistant *S. aureus* (MRSA). It is noteworthy that the HDA derivative compounds (MA-HDA and OA-HDA) increased their antimicrobial activity and reduced the MIC_{50} against MRSA by 66% and 87%, respectively (MIC_{50} of 25 and 10 μg/mL) compared to their original compounds (OA and MA, MIC_{50} 75 μg/mL). The same behavior was seen with the DAD derivative compounds (MA-DAD and OA-DAD), which reduced MRSA MIC_{50} by 66% and 60%, respectively. Since antibiotic-resistant bacteria like MRSA are nowadays a public health concern, it is crucial to find new antimicrobials that do not produce resistance mechanisms in these bacteria. Thus, the improved activity of HDA and DAD compounds and the fact that resistance mechanisms have not yet been found in the parent compounds MA and OA[12,16] identify these molecules as a possible good alternative for MRSA treatment.

Additional studies were performed to determine their in vitro toxicity using the A549 human epithelial pulmonary cell line. The in vitro toxicity in cells, expressed in Table 1 as the concentration that kills 50% of the cells (CC_{50}), demonstrates that the HDA and the DAD derivatives from MA and OA were not more toxic than their precursors, although they showed better antimicrobial activity in some bacterial strains.

DOI: 10.1021/acsinfecdis.9b00125
ACS Infect. Dis. 2019, 5, 1581−1589

In Vivo Toxicity and Efficacy in *Galleria mellonella*. *Galleria mellonella* was used to evaluate the toxicity (lethal dose) of the new antimicrobial compounds tested.[20] We evaluated the compound dose per kilogram of greater wax moth larvae that kills 50% of the animal population (lethal dose 50, LD_{50}). Using the MIC_{50} and the toxicity indexes CC_{50} and LD_{50}, the selectivity indexes (SI) were calculated. The selectivity indexes (in cells or *Galleria mellonella*) emphasize the improvement of the HDA derivatives' activity (OA-HDA, SI = 62.2 or 1313; MA-HDA, SI = 17.9 or 661) against *S. aureus* growth related to their toxicity, as seen with the 5-fold increase in the SI of OA-HDA compared to OA.

The use of *Galleria mellonella* as an invertebrate animal model to test in vivo toxicity and to calculate the SI is crucial because the selectivity index (SI) is increased considerably when calculated with the LD_{50} rather than with the CC_{50} (Table 1). In some cases, the toxicity in vivo can be significantly different; for example, the toxicity of the MA-HDA compound increased in vitro while the in vivo toxicity decreased in comparison to the predecessor MA. Our results highlight the use of an animal model for toxicity evaluation to better select a compound for further investigative steps or drug development. The use of *G. mellonella* is a cheap screening alternative for in vivo toxicity and efficacy prior to analysis in rodents or even more expensive options.

Additionally, *Galleria mellonella* larvae were used as a *S. aureus* model of infection to evaluate in vivo antibacterial efficacy of the best active amide derivatives (MA-HDA and OA-HDA). *G. mellonella* were infected with *S. aureus* at 1.5×10^9 cfu/mL into the hemocoel and treated twice with the compounds at 240 mg/kg (1 and 6 h post-infection). As illustrated in Figure 1, treatment with MA-HDA and MA

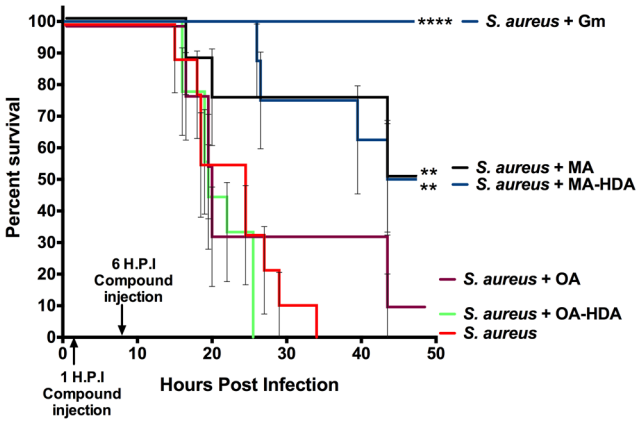

Figure 1. Kaplan–Meier survival curve of *Galleria mellonella* larvae infected with *S. aureus* and treated with the different compounds 1 and 6 h post-infection at a final concentration of 240 mg per kg of body weight. Gentamicin (Gm) at 20 mg/kg was used as a control. Asterisks: statistically significant difference versus *S. aureus* without treatment in a log-rank test, GraphPad 6.0 (**: *p*-value <0.005; ****: *p*-value <0.0001).

compounds resulted in 50% of the larvae surviving, whereas only 20% of *Galleria* survived the *S. aureus* infection after the treatment with OA. Nevertheless, no differences were seen between the untreated insects and the ones treated with OA-HDA, showing a lack of in vivo activity of this compound. As the in vivo toxicity diminished in the MA-HDA derivative, these results enhanced the antibacterial efficacy of MA-HDA by increasing the survival of *Galleria mellonella* infected with *S. aureus* by 50%.

Since these two new compounds (MA-HDA and OA-HDA) have high activity and selectivity index, they could be considered good antibacterial agents in a modern therapy context, especially useful in the treatment of multidrug resistant bacteria. As the antibiotics used in chemotherapy no longer appear to be as effective as they were when created, there is an urgent need for the discovery of new antibacterial drugs with different action mechanisms to tackle the growing drug resistance.

Effect on Bacterial Cell Membrane and Possible Mechanisms of Action. To identify a preliminary mechanism of action of the different compounds used in this work, Live/Dead and membrane damage staining analyses were first carried out. The Live/Dead analysis (Figure 2A) was performed by staining *S. aureus* cells after 4 h of treatment with the diverse compounds. This differential staining allowed discrimination of viable bacteria (stained with SYTO9 dye, green) from dead bacteria (stained with PI dye, red), as well as seeing the growth impairment that the treatment could cause. After 4 h of treatment, a notable decrease of viable cells could be detected when the OA, MA, OA-HDA, MA-HDA, OA-DAD, and MA-DAD compounds were used, as shown in Figure 2A with the average count in Table S1, while a persistence of these cells was seen when compounds without activity were used (MA-HDA-MA and MA-DMPA). Moreover, a specific membrane staining with FM 4-64 dye was performed. After staining for 10 min (Figure 2B), membrane impairment in the active compounds could be observed. Some dye accumulations could be appreciated in the membrane (red dots indicated by an arrow) when treated with the active antimicrobial compounds (OA, MA, OA-HDA, MA-HDA, OA-DAD, and MA-DAD). These accumulations reaffirmed the Live/Dead results and suggested a bacteriolytic mode of action.

Finally, scanning electron microscope (SEM) characterization of the treated *S. aureus* cells was carried out to validate our previous staining experiments. Figure 2C shows SEM images of *S. aureus* cells after exposure to the compounds. The images show that the bacteria's surface became rough and bubbly in many *S. aureus* treated cells while the nontreated cells' membrane remained smooth, thus suggesting membrane damage and further corroborating the results seen in the fluorescent microscope analysis.

Previous results show that MA and OA induced cell membrane destabilization and destruction.[12,21] Proteases, protein kinases, and transcription factors have been proposed as a target for these compounds,[10,22−25] but the exact molecular mechanism remains unknown. The mechanism of action of MA has not been reported in bacteria but only against protozoa, nematodes, viruses, and cancerogenic cells as a glycogen phosphorylase inhibitor,[26] regulator of transcription factors and protein kinases,[24] and inhibitor of proteases.[27,28] However, a nonstandard binding mechanism of MA to these proteins[29] has also been suggested.

Regarding the mechanism of action of OA against bacteria, it is well-known that it inhibits peptidoglycan metabolism and prevents cell division in *Listeria monocytogenes*.[18] Other studies demonstrate a similar effect of OA in the Gram-positive *Streptococcus mutans* by proving the effect in both the peptidoglycan metabolism at a transcriptional level[10] and the adherence to the tooth surface to form the cariogenic

DOI: 10.1021/acsinfecdis.9b00125
ACS Infect. Dis. 2019, 5, 1581−1589

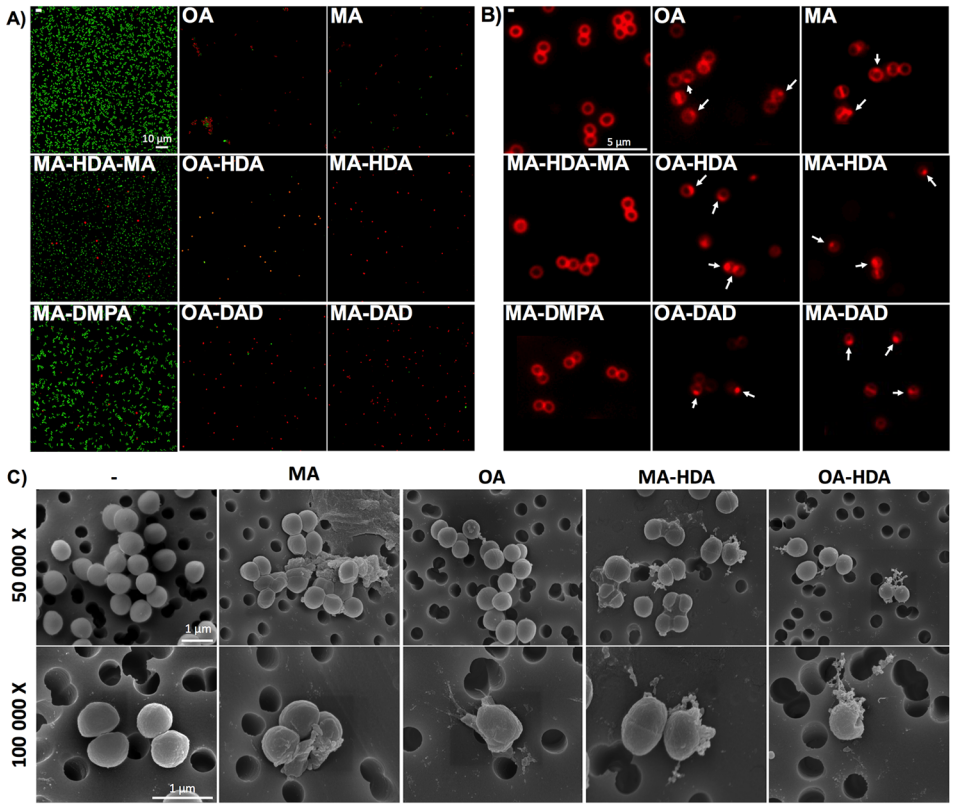

Figure 2. (A) Live/Dead analysis in *S. aureus*. Green fluorescence indicates live cells and red fluorescence indicates metabolically inactive (dead) cells. (B) Membrane damage analysis by FM 4-64 staining of *S. aureus*. The arrows show nonuniform stain accumulations in the membrane indicating cell damage. (C) SEM images of *S. aureus* cells after the compounds' treatment.

biofilm.[30] Despite not having antimicrobial activity in *Escherichia coli*, it has been demonstrated that OA affects the efflux of pumps in this bacteria[23] and acts as a stress inducer agent[22] that reduces the expression of the cysteine regulon and induces heat shock response with the DnaK synthesis.

Nevertheless, the different activity among the OA and MA derivatives and concerning the parent OA and MA compounds suggests that the mechanism of action of these derivatives might be different from the natural triterpenic acids. The only structural difference between all the derivatives is the length of the diamine residue. It seems that these compounds require a certain chain length to be active, and for this reason, only the longer chain (HDA and DAD) derivatives are active. This might have some justification if the mechanism of action is due to bacterial cell membrane interaction and posterior destabilization, as suggested by the Live/Dead and membrane damage staining analyses and the SEM characterization. Both Gram-positive and Gram-negative bacteria have a negatively charged envelope due to the negative charge of teichoic acids and lipopolysaccharides, respectively, but regarding the plasma membrane, Gram-positive bacteria contain a larger portion of negatively charged phospholipids than Gram-negative bacteria.[31] At a physiological pH, the terminal amine group is positively charged and can promote the interaction of the derivatives with the plasma membrane by electrostatic interactions which are going to be enhanced in the Gram-positive membrane. Once the derivatives are in contact with the membrane, they need to be inserted efficiently to produce membrane destabilization. This second step is where the length of the alkyl chain may have relevant importance. If the alkyl chain is short, the interaction is mainly superficial, and the derivatives do not have the possibility of being inserted into the cell membrane. On the other hand, if the length of the chain is long enough, the derivatives can be inserted into the cell membrane, thus provoking disruption. It is known that the alkyl chain length in small organic compounds which tackle bacterial cell membranes has a major impact on the activity of the compounds.[32−34] In our case, HDA-derivatives, having a diamine alkyl chain of 6 carbons, present the most effective combination.

Antibiofilm Activity against *Staphylococcus aureus* Static and Continuous Biofilms. Since bacteria within biofilms can be more resistant to antimicrobials than in planktonic state, the removal capacity of preformed *S. aureus* biofilms grown in static and continuous flow was tested.

First, we grew a *S. aureus* biofilm on catheter tubes for 72 h. Then, we treated them with different compounds at a concentration of 50 μg/mL for an additional 24 h. As we can see in Figure 3, the more active compounds (MA, MA-HDA, and OA-HDA) were able to remove more than 99% of the preformed biofilm when compared to the untreated biofilm. However, at the concentration tested, OA and MA-HDA-MA had subinhibitory concentration activity (Figure 3) without any ability to remove the biofilm, but they do enhance the formation of the biofilm[35] which could explain the increase in the biofilm growth produced. Note that the antibacterial activity was higher for the MA-HDA and OA-HDA compounds in contrast to the well-known antibiotic ciprofloxacin.

Second, we performed a continuous *S. aureus* flow biofilm to resemble the conditions in which this bacteria establishes a chronic infection. The *S. aureus* continuous biofilm was formed

DOI: 10.1021/acsinfecdis.9b00125
ACS Infect. Dis. 2019, 5, 1581−1589

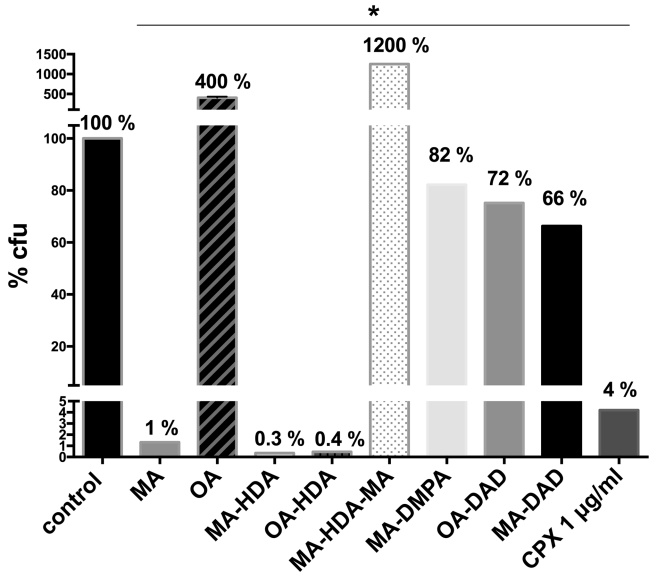

Figure 3. Antibacterial efficacy of compounds on *S. aureus* ATCC 12600 catheter biofilms. Bars indicate percentage (%) of viable biofilm cells (cfu) remaining on the catheter after 24 h treatment with the compounds. Cpx, ciprofloxacin. Asterisk (*): statistically significant difference versus control without treatment (p-value <0.05 in an unpaired t-test, GraphPad 6.0).

during 4 consecutive days and afterward treated with different compounds at a concentration of 50 μg/mL for an additional 24 h. The images of Figure 4A are confocal Z-projections with the corresponding orthogonal views of the biofilm after treatment and the plot in Figure 4B shows the average biofilm biomass. Clearly, the best antibiofilm activity was detected with the MA-HDA and OA-HDA compounds (30% and 45% reduction in biofilm biomass, respectively) with a corresponding decrease in thickness (around 10 μm) as seen in the orthogonal views (Figure 4A and B). It is important to point out that these compounds have better antimicrobial efficacy compared to the MA and OA original compounds.

CONCLUSIONS

For the first time, novel OA and MA derivatives outperform the known antimicrobial activity of their parent compounds. Of the 14 OA and MA C-28 amide derivatives studied, two derivatives, MA-HDA and OA-HDA, have shown better in vitro antimicrobial activity in all of the Gram-positive bacterial strains tested by significantly reducing the MIC_{50} against MRSA in 66% and 87%, respectively, when compared to the MA and OA compounds. In vitro toxicity studies also showed that these new derivatives did not increase the toxicity with respect to their parent compounds. Preliminary studies conducted to shed light on their mechanism of action revealed that these compounds were able to penetrate and damage the bacterial cellular membrane. These excellent in vitro results have also been validated in vivo in a *Galleria mellonella* animal model. In particular, MA-HDA showed the best results in terms of efficacy and toxicity, increasing the survival of *G. mellonella* infected with *S. aureus* by 50%.

Taken together, these results point out the relevance that natural feedstock has in providing bioactive compounds for therapeutic purposes. In this case, OA and MA are natural products obtained in large quantities from olive oil waste, and therefore, they are easily accessible and inexpensive. Through very few steps of very simple chemical transformations, we have obtained novel derivatives that are highly active in vitro and in vivo against dangerous Gram-positive bacterial strains including MRSA. Their mechanism of action suggests that these compounds could be used in combination with other antibiotics to promote synergy.

EXPERIMENTAL SECTION

Chemistry. Oleanolic (3β-hydroxyolean-12-en-28-oic acid, OA) and maslinic (2α,3β-dihydroxyolean-12-en-28-oic acid) acids were isolated from solid waste resulting from olive oil production, which were extracted in a Soxhlet with hexane and EtOAc successively.[36] Both acids were purified from these mixtures by flash chromatography over silica gel, eluting with CH_2Cl_2/acetone of increasing polarity.[37] The C-28 amide derivatives were prepared following a protocol previously described (see Scheme 1).[13] Very briefly, the carboxyl group of the OA and MA was first activated with *O*-(Benzotriazol-1-yl)-*N*,*N*,*N*′,*N*′-tetramethyluronium tetrafluoroborate (TBTU). The OA and MA-TBTU derivatives were obtained by the addition of TBTU in the presence of diisopropylethylamine (DIEA) in dry THF and at room temperature. Second, the OA and MA-TBTU derivatives were dissolved in CH_2Cl_2 and reacted with the corresponding diamine reagents [propane-1,3-

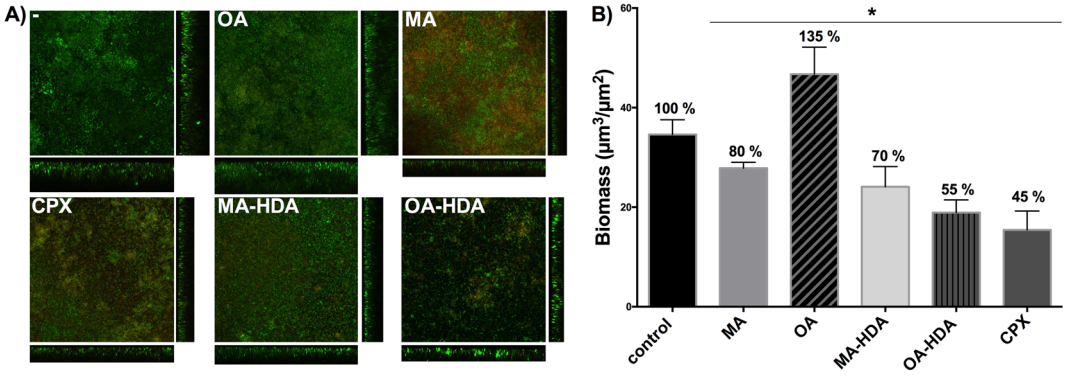

Figure 4. Antibiofilm efficacy of 24 h treatment of compounds against *S. aureus* biofilms grown on a continuous flow system for 96 h. (A) Confocal laser scanning microscope (CLSM) pictures (sum of stack images and orthogonal views) stained with LIVE/DEAD BacLight Bacterial Viability Kit. (B) Biomass ($\mu m^3/\mu m^2$) of the biofilms analyzed with COMSTAT2. Cpx, ciprofloxacin. Asterisk (*): statistically significant difference versus control without treatment (p-value <0.05 in an unpaired t-test, GraphPad 6.0).

DOI: 10.1021/acsinfecdis.9b00125
ACS Infect. Dis. 2019, 5, 1581−1589

diamine (PDA), hexane-1,6-diamine (HDA), and decane-1,10-diamine (DAD)] in the presence of K_2CO_3 to originate two products in all cases: monomers exceeding 60% yield (MA-PAD 63%, MA-HDA 64%, MA-DAD 62%, OA-PAD 65%, OA-HDA 62%, and OA-DAD 63%) and dimers close to 30% yield (MA-PAD-MA 27%, MA-HDA-MA 28%, MA-DAD-MA 30%, OA-PAD-OA 28%, OA-HDA-OA 29%, and OA-DAD-OA 29%).[13] The reaction of OA and MA-TBTU derivatives with *N,N*-dimethyl-1,3-propanediamine afforded only one compound (MA-DMPA and OA-DMPA) with a 90% yield in both cases. In all instances, the compounds were purified by column chromatography. The purity of the compounds was determined by a Waters Acquity UPLC system (ultra-performance liquid chromatography) coupled with a Waters Synapt G2 HRMS spectrometer (high resolution mass spectra), with ESI (electrospray ionization) being ⩾95%. Isolated compounds were characterized by ^{1}H NMR and HRMS, matching what has already been reported. MA-DMPA and OA-DMPA were characterized by ^{1}H and ^{13}C NMR and HRMS. Copies of NMR spectra and HRMS values are included in the Supporting Information.

Bacterial Strains and Growth Conditions. Wild-type *Staphylococcus aureus* CECT 86 (ATCC 12600), *Staphylococcus epidermidis* CECT 231 (ATCC 1798), *Streptococcus mutans* CECT 479 (ATCC 25175), *Enterococcus faecalis* CECT 481 (ATCC 19433), *Escherichia coli* K12 MG1655 CECT 433 (ATCC 700926), and *Pseudomonas aeruginosa* PAO1 CECT 4122 (ATCC 15692) were obtained from the Spanish Type Culture Collection (CECT). *Staphylococcus aureus* MRSA was from our laboratory stock.[38] *S. aureus* antimicrobial activity profiles are listed in Table S2. All strains were routinely cultivated in Tryptic Soy Broth (TSB) or Luria−Bertani (LB) medium (Scharlab) at 37 °C.

Antibacterial Susceptibility Testing (In Vitro Activity). The different compounds were tested against different bacterial strains as previously described.[38] Briefly, bacteria were grown in TSB or LB medium to an $O.D._{550} \approx 0.1$ ($\approx(4.3 \times 10^7) \pm (1.4 \times 10^6)$ cfu/mL) and plated in a 96-well microtiter plate (Corning 3596 Polystyrene Flat Bottom 96 Well, Corning NY) containing several concentrations of the compounds according to the Clinical Laboratory Standards Institute (CLSI) guidelines.[39] The plate was incubated at 37 °C with shaking at 120 rpm for 8 h and the absorbance at 550 nm was read every 15 min in a SPARK Multimode microplate reader (Tecan).

The minimal inhibitory concentration 50% (MIC_{50}) was defined as the compound concentration that inhibited the bacterial growth by 50%.

Mammalian Cytotoxicity Determination (In Vitro Toxicity). Human alveolar epithelial A549 cells (ATCC CCL-185) were set and allowed to sediment in a microtiter plate (Corning 3596 Polystyrene Flat Bottom 96 Well, Corning NY) at 2×10^4 cells/well and compounds were added at several concentrations. After 24 h, a 10% of MTT solution (3-[4,5-dimethylthiazol-2-yl]-2,5-diphenyltetrazolium bromide, Sigma-Aldrich) was added and the formazan that precipitated 3 h later was dissolved with acidic isopropanol. Absorbance was read at 550 nm in a SPARK multimode microplate reader (Tecan) to determine cell viability. CC_{50} was calculated with Prism 6.00 (GraphPad Software) as the concentration of the compound that diminished the cell population by 50%. Values ± standard deviation for 3 independent experiments are shown.

Animal Toxicity Determination (In Vivo Toxicity). *Galleria mellonella* larvae were reared on an artificial diet (15% corn flour, 15% wheat flour, 15% baby cereal, 11% powdered milk, 6% brewer's yeast, 25% honey, and 13% glycerol) at 34 °C in darkness prior to use. *G. mellonella* larvae were injected with 10 μL of each compound at 300 and 400 mg/kg with a microsyringe (Hamilton) into the hemocoel through the top left proleg. Five larvae (200−250 mg each) were injected per compound and concentration and larvae mortality was recorded daily. Control groups were injected with 10 μL of 1× PBS (Phosphate Saline Buffer) or the vehicle (DMSO) at the highest concentration used.

LD_{50} (median lethal dose) was calculated with Prism 6.00 (GraphPad Software) as the concentration of the compound that killed 50% of the larvae within 24 h. Values ± standard deviation for 3 independent experiments are shown.

Survival Assay in *Galleria mellonella* Animal Model (In Vivo Efficacy). An infective dose of *S. aureus* (1.5×10^9 cfu/mL) was injected in *Galleria mellonella* larvae into the hemocoel through the upper left proleg. One hour and six hours post-infection, 10 μL of the compound at 240 mg/kg were injected through a different proleg. Each compound was injected in a group of five larvae (200−250 mg each). Control groups were injected with 10 μL of 1× PBS (Phosphate Saline Buffer), the vehicle (DMSO), or gentamicin at 20 mg/kg. *G. mellonella* larvae were incubated at 37 °C and mortality was recorded daily. Survival curves were plotted using Kaplan−Meier analysis and differences in survival rates were analyzed by the log-rank test (GraphPad Prism 6.00). Differences with P values of <0.005 were considered statistically significant.

Fluorescent Microscopy Viability and Membrane Analysis. *S. aureus* was grown in TSB medium to an $O.D._{550} \approx 0.3$ ($\approx(1.3 \times 10^8) \pm (3 \times 10^7)$ cfu/mL) and the compounds were added at a concentration of 50 μg/mL for 4 h in the live−dead test and for 10 min in the membrane analysis.

The bacterial cells were harvested and stained with the LIVE/DEAD BactLight Bacterial Viability kit (Thermo Fisher Scientific) for the viability test and with 10 μg/mL of *N*-(3-triethylammoniumpropyl)-4-(6-(4-(diethylamino)phenyl)-hexatrienyl)pyridinium dibromide (FM 4−64, Thermo Fisher Scientific) for the membrane analysis, according to the manufacturer's specifications. Bacteria were then visualized with a Nikon inverted fluorescent microscope ECLIPSE Ti−S/L100 (Nikon) coupled with a DS-Qi2 Nikon camera (Nikon).

Scanning Electronic Microscopy (SEM) Bacterial Analysis. Morphological analysis of *S. aureus* after exposure to antimicrobial compounds was performed using field emission scanning electron microscopy (Nova NanoSEM FEISEM). *S. aureus* was grown in TSB medium to an $O.D._{550} \approx 0.6$ ($\approx(2 \times 10^8) \pm (4 \times 10^7)$ cfu/mL) and exposed to compounds at a concentration of 25 μg/mL for 30 min. Nonexposed bacteria were used as a reference. Immediately after exposure, bacteria were fixed in glutaraldehyde. For that purpose, 100 μL of treated culture were centrifuged for 5 min at 6000 rpm and TSB was replaced with 50 μL of glutaraldehyde solution (3 wt.%). After 3 h at room temperature, the fixative was replaced with the same volume of fresh fixative and left at 4 °C overnight. Fixed bacteria were deposited on the top of the porous membranes by filtration in soft vacuum. To remove the fixative, deposited bacteria were washed three times with 1× PBS (during 15 min for each replacement) and dehydrated in serially diluted ethanol (30,

DOI: 10.1021/acsinfecdis.9b00125
ACS Infect. Dis. 2019, 5, 1581−1589

50, 70, 90, and 100 wt.%) (30 min in each concentration). The cells in ethanol were finally dried using critical point technique (CPD Baltec 030). Before examination in SEM, bacteria deposited on membranes were sputtered with a thin layer of gold for better conductivity.

Antibacterial Effect of Compounds on Biofilms Growing on Catheters. Sterile silicone catheter pieces (2 mm diameter and 1 cm width) (SILT-002, SUDELAB) were placed in a 10 mL tube and covered with a *S. aureus* culture of $O.D._{550} \approx 0.1$ ($\approx(4.3 \times 10^7) \pm (1.43 \times 10^6)$ cfu/mL) in TSB medium +0.2% glucose. The tubes were incubated at 37 °C without shaking. After 72 h, the catheter pieces were washed three times with 1× phosphate buffer saline (PBS) (Fisher BioReagents) to discard the planktonic growth (nonbiofilm forming bacteria) and were treated with the different compounds at a concentration of 50 μg/mL. After 24 h, the catheters were washed again and a solution of 1× PBS + TWEEN 0.05% was added. Then, the tubes were placed in an ultrasonic bath (USC100T, VWR) for 5 min and vortexed for 30 s to remove the bacteria growing in a biofilm. Serial dilutions were plated on TSB agar plates to determine the viable cells in the biofilm (cfu, colony forming units). The viable counts in the control experiment without treatment were $(4.4 \times 10^5) \pm (1.7 \times 10^5)$ cfu/mL.

Antibacterial Effect of Compounds on Continuous-Flow Biofilms. *S. aureus* continuous-flow biofilms were formed as previously described[40,41] with some modifications and with an initial bacteria inoculum of $O.D._{550} \approx 0.1$ ($\approx(4.3 \times 10^7) \pm (1.43 \times 10^6)$ cfu/mL). The biofilms were grown in 2% (v/v) TSB + 0.2% glucose pumped through the flow cells chambers using a peristaltic pump ISM (Ismatec) at 42 μL/min. These flow cells (DTU) were previously coated with 20% bovine plasma (Biowest) overnight prior to the inoculation of the bacteria. After 4 days of growth, the flow was stopped and different compounds diluted in media, including ciprofloxacin as a control, were injected into the formed biofilms. After 24 h treatment, biofilms were stained with the Live/Dead BacLight Bacterial Viability Kit (Thermo Fisher Scientific) and visualized under a Zeiss LSM 800 confocal laser scanning microscope (CLSM) with the 20×/0.8 air objective. Analysis of the images obtained was performed to quantify the biomass and thickness of the biofilms using ImageJ FIJI and COMSTAT2 software.[42]

■ ASSOCIATED CONTENT

Supporting Information

The Supporting Information is available free of charge on the ACS Publications website at DOI: 10.1021/acsinfecdis.9b00125.

General information and copies of NMR spectra and HRMS values (PDF)

■ AUTHOR INFORMATION

Corresponding Authors

*E-mail: lac@ugr.es.
*E-mail: etorrents@ibecbarcelona.eu.

ORCID

Andrés Parra: 0000-0001-7485-8753
Luis Álvarez de Cienfuegos: 0000-0001-8910-4241
Eduard Torrents: 0000-0002-3010-1609

Author Contributions

The manuscript was written through contributions of all authors. All authors have given approval to the final version of the manuscript. Karina Vega Granados and Andrés Parra designed and synthesized the library of oleanolic and maslinic acid derivatives and wrote the manuscript. Núria Blanco-Cabra, Laura Moya-Andérico, and Marija Vukomanovic performed biological assays and wrote the manuscript. Eduard Torrents and Luis Alvarez de Cienfuegos directed the research, revised the experimental data, and wrote the manuscript. All authors have given approval to the final version of the manuscript.

Notes

The authors declare no competing financial interest.

■ ACKNOWLEDGMENTS

This study was partially supported by grants from the Ministerio de Economía, Industria y Competitividad, MINECO, and Agencia Estatal de Investigación, AEI, Spain, cofunded by Fondo Europeo de Desarrollo Regional, FEDER, European Union (BIO2015−63557-R, FIS2017−85954-R and RTI2018−098573-B-100), the CERCA program and *AGAUR-Generalitat de Catalunya* (2017SGR-1079), the European Regional Development Fund (FEDER), Catalan and Spanish cystic fibrosis federation, the EIT Health and Obra Social "La Caixa". K.V.G. thanks CONACYT (Consejo Nacional de Ciencia y Tecnología) Gobierno del estado de Baja California 2015 for her fellowship. The authors wish to thank Johanna Binding and Zoe Downer for technical assistance. L.A.C. wants to thank "Unidad de Excelencia Química aplicada a Biomedicina y Medioambiente" for support. Finally we would like to thank the Editor and reviewers whose suggestions greatly improved the manuscript.

■ REFERENCES

(1) Otto, M. (2018) Staphylococcal Biofilms. *Microbiol. Spectrum 6* (4), 1 DOI: 10.1128/microbiolspec.GPP3-0023-2018.
(2) Stewart, P. S., and Costerton, J. W. (2001) Antibiotic resistance of bacteria in biofilms. *Lancet 358* (9276), 135−8.
(3) Costerton, J. W., Stewart, P. S., and Greenberg, E. P. (1999) Bacterial biofilms: a common cause of persistent infections. *Science 284* (5418), 1318−22.
(4) Hassoun, A., Linden, P. K., and Friedman, B. (2017) Incidence, prevalence, and management of MRSA bacteremia across patient populations-a review of recent developments in MRSA management and treatment. *Crit Care 21* (1), 211.
(5) Tong, S. Y., Davis, J. S., Eichenberger, E., Holland, T. L., and Fowler, V. G., Jr. (2015) *Staphylococcus aureus* infections: epidemiology, pathophysiology, clinical manifestations, and management. *Clin. Microbiol. Rev. 28* (3), 603−61.
(6) Suresh, M. K., Biswas, R., and Biswas, L. (2019) An update on recent developments in the prevention and treatment of *Staphylococcus aureus* biofilms. *Int. J. Med. Microbiol. 309*, 1.
(7) Jesus, J. A., Lago, J. H., Laurenti, M. D., Yamamoto, E. S., and Passero, L. F. (2015) Antimicrobial activity of oleanolic and ursolic acids: an update. *Evid Based Complement Alternat Med. 2015*, 620472.
(8) Rufino-Palomares, E. (2015) Anti-cancer and Anti-angiogenic Properties of Various Natural Pentacyclic Tri-terpenoids and Some of their Chemical Derivatives. *Curr. Org. Chem. 19* (10), 1.
(9) Fernández-Hernández, A., Martinez, A., Rivas, F., García-Mesa, J. A., and Parra, A. (2015) Effect of the Solvent and the Sample Preparation on the Determination of Triterpene Compounds in Two-Phase Olive-Mill-Waste Samples. *J. Agric. Food Chem. 63* (17), 4269−4275.

DOI: 10.1021/acsinfecdis.9b00125
ACS Infect. Dis. 2019, 5, 1581−1589

(10) Park, S. N., Ahn, S. J., and Kook, J. K. (2015) Oleanolic acid and ursolic acid inhibit peptidoglycan biosynthesis in *Streptococcus mutans* UA159. *Braz J. Microbiol 46* (2), 613−7.
(11) Fontanay, S., Grare, M., Mayer, J., Finance, C., and Duval, R. E. (2008) Ursolic, oleanolic and betulinic acids: antibacterial spectra and selectivity indexes. *J. Ethnopharmacol. 120* (2), 272−6.
(12) Kim, S., Lee, H., Lee, S., Yoon, Y., and Choi, K. H. (2015) Antimicrobial action of oleanolic acid on *Listeria monocytogenes*, *Enterococcus faecium*, and *Enterococcus faecalis*. *PLoS One 10* (3), No. e0118800.
(13) Medina-O'Donnell, M., Rivas, F., Reyes-Zurita, F. J., Martinez, A., Lupianez, J. A., and Parra, A. (2018) Diamine and PEGylated-diamine conjugates of triterpenic acids as potential anticancer agents. *Eur. J. Med. Chem. 148*, 325−336.
(14) Liu, J. (1995) Pharmacology of oleanolic acid and ursolic acid. *J. Ethnopharmacol. 49* (2), 57−68.
(15) Lozano-Mena, G., Sanchez-Gonzalez, M., Juan, M. E., and Planas, J. M. (2014) Maslinic acid, a natural phytoalexin-type triterpene from olives–a promising nutraceutical? *Molecules 19* (8), 11538−59.
(16) Garcia-Salinas, S., Elizondo-Castillo, H., Arruebo, M., Mendoza, G., and Irusta, S. (2018) Evaluation of the Antimicrobial Activity and Cytotoxicity of Different Components of Natural Origin Present in Essential Oils. *Molecules 23* (6), 1399.
(17) Abreu, A. C., Paulet, D., Coqueiro, A., Malheiro, J., Borges, A., Saavedra, M. J., Choi, Y. H., and Simões, M. (2016) Antibiotic adjuvants from *Buxus sempervirens* to promote effective treatment of drug-resistant *Staphylococcus aureus* biofilms. *RSC Adv. 6* (97), 95000−95009.
(18) Kurek, A., Grudniak, A. M., Szwed, M., Klicka, A., Samluk, L., Wolska, K. I., Janiszowska, W., and Popowska, M. (2010) Oleanolic acid and ursolic acid affect peptidoglycan metabolism in *Listeria monocytogenes*. *Antonie van Leeuwenhoek 97* (1), 61−8.
(19) Pavel, I. Z., Danciu, C., Oprean, C., Dehelean, C. A., Muntean, D., Csuk, R., and Muntean, D. M. (2016) In Vitro Evaluation of the Antimicrobial Ability and Cytotoxicity on Two Melanoma Cell Lines of a Benzylamide Derivative of Maslinic Acid. *Anal. Cell. Pathol. 2016*, 2787623.
(20) Ignasiak, K., and Maxwell, A. (2017) *Galleria mellonella* (greater wax moth) larvae as a model for antibiotic susceptibility testing and acute toxicity trials. *BMC Res. Notes 10* (1), 428.
(21) Martin-Navarro, C. M., Lopez-Arencibia, A., Sifaoui, I., Reyes-Batlle, M., Fouque, E., Osuna, A., Valladares, B., Pinero, J. E., Hechard, Y., Maciver, S. K., and Lorenzo-Morales, J. (2017) Amoebicidal Activity of Caffeine and Maslinic Acid by the Induction of Programmed Cell Death in *Acanthamoeba*. *Antimicrob. Agents Chemother. 61* (6), 1 DOI: 10.1128/AAC.02660-16.
(22) Grudniak, A. M., Kurek, A., Szarlak, J., and Wolska, K. I. (2011) Oleanolic and ursolic acids influence affect the expression of the cysteine regulon and the stress response in *Escherichia coli*. *Curr. Microbiol. 62* (4), 1331−6.
(23) Martins, A., Vasas, A., Viveiros, M., Molnar, J., Hohmann, J., and Amaral, L. (2011) Antibacterial properties of compounds isolated from *Carpobrotus edulis*. *Int. J. Antimicrob. Agents 37* (5), 438−44.
(24) Sharma, H., Kumar, P., Deshmukh, R. R., Bishayee, A., and Kumar, S. (2018) Pentacyclic triterpenes: New tools to fight metabolic syndrome. *Phytomedicine 50*, 166−177.
(25) Liang, Z., Zhang, L., Li, L., Liu, J., Li, H., Zhang, L., Chen, L., Cheng, K., Zheng, M., Wen, X., Zhang, P., Hao, J., Gong, Y., Zhang, X., Zhu, X., Chen, J., Liu, H., Jiang, H., Luo, C., and Sun, H. (2011) Identification of pentacyclic triterpenes derivatives as potent inhibitors against glycogen phosphorylase based on 3D-QSAR studies. *Eur. J. Med. Chem. 46* (6), 2011−21.
(26) Mukaratirwa, S., Gcanga, L., and Kamau, J. (2016) Efficacy of maslinic acid and fenbendazole on muscle larvae of *Trichinella zimbabwensis* in laboratory rats. *J. Helminthol. 90* (1), 86−90.
(27) Moneriz, C., Marin-Garcia, P., Garcia-Granados, A., Bautista, J. M., Diez, A., and Puyet, A. (2011) Parasitostatic effect of maslinic acid. I. Growth arrest of *Plasmodium falciparum* intraerythrocytic stages. *Malar. J. 10*, 82.
(28) De Pablos, L. M., dos Santos, M. F., Montero, E., Garcia-Granados, A., Parra, A., and Osuna, A. (2010) Anticoccidial activity of maslinic acid against infection with *Eimeria tenella* in chickens. *Parasitol. Res. 107* (3), 601−4.
(29) Moneriz, C., Mestres, J., Bautista, J. M., Diez, A., and Puyet, A. (2011) Multi-targeted activity of maslinic acid as an antimalarial natural compound. *FEBS J. 278* (16), 2951−61.
(30) Kozai, K., Miyake, Y., Kohda, H., Kametaka, S., Yamasaki, K., Suginaka, H., and Nagasaka, N. (1987) Inhibition of glucosyltransferase from *Streptococcus mutans* by oleanolic acid and ursolic acid. *Caries Res. 21* (2), 104−8.
(31) Malanovic, N., and Lohner, K. (2016) Gram-positive bacterial cell envelopes: The impact on the activity of antimicrobial peptides. *Biochim. Biophys. Acta, Biomembr. 1858* (5), 936−46.
(32) Ghosh, C., Manjunath, G. B., Akkapeddi, P., Yarlagadda, V., Hoque, J., Uppu, D. S., Konai, M. M., and Haldar, J. (2014) Small molecular antibacterial peptoid mimics: the simpler the better! *J. Med. Chem. 57* (4), 1428−36.
(33) Hoque, J., Konai, M. M., Sequeira, S. S., Samaddar, S., and Haldar, J. (2016) Antibacterial and Antibiofilm Activity of Cationic Small Molecules with Spatial Positioning of Hydrophobicity: An in Vitro and in Vivo Evaluation. *J. Med. Chem. 59* (23), 10750−10762.
(34) Konai, M. M., and Haldar, J. (2017) Fatty Acid Comprising Lysine Conjugates: Anti-MRSA Agents That Display In Vivo Efficacy by Disrupting Biofilms with No Resistance Development. *Bioconjugate Chem. 28* (4), 1194−1204.
(35) Kaplan, J. B. (2011) Antibiotic-induced biofilm formation. *Int. J. Artif. Organs 34* (9), 737−51.
(36) Garcia-Granados, A. Process for the industrial recovery of oleanolic and maslinic acids contained in the olive milling byproducts. PCT Int. Appl. WO 9804331, 1998.
(37) Martinez, A., Perojil, A., Rivas, F., Parra, A., Garcia-Granados, A., and Fernandez-Vivas, A. (2015) Biotransformation of oleanolic and maslinic methyl esters by *Rhizomucor miehei* CECT 2749. *Phytochemistry 117*, 500−508.
(38) Barniol-Xicota, M., Escandell, A., Valverde, E., Julian, E., Torrents, E., and Vazquez, S. (2015) Antibacterial activity of novel benzopolycyclic amines. *Bioorg. Med. Chem. 23* (2), 290−6.
(39) Clinical and laboratory standards institute (2006) *Methods for dilution andtimicrobial susceptibility test for bacteria that grow aerobically; approved standard*, CLSI document M7-A7, 7th ed.;, Clinical and Laboratory Standards Institute, Wayne, PA.
(40) Baelo, A., Levato, R., Julian, E., Crespo, A., Astola, J., Gavalda, J., Engel, E., Mateos-Timoneda, M. A., and Torrents, E. (2015) Disassembling bacterial extracellular matrix with DNase-coated nanoparticles to enhance antibiotic delivery in biofilm infections. *J. Controlled Release 209*, 150−8.
(41) Crespo, A., Blanco-Cabra, N., and Torrents, E. (2018) Aerobic Vitamin B12 Biosynthesis Is Essential for *Pseudomonas aeruginosa* Class II Ribonucleotide Reductase Activity During Planktonic and Biofilm Growth. *Front. Microbiol. 9*, 986.
(42) Givskov, M., Hentzer, M., Ersbøll, B. K.ær, Heydorn, A., Sternberg, C., Nielsen, A. T., and Molin, Sør. (2000) Quantification of biofilm structures by the novel computer program COMSTAT. *Microbiology 146*, 2395−407.

DOI: 10.1021/acsinfecdis.9b00125
ACS Infect. Dis. 2019, 5, 1581−1589

Novel Oleanolic and Maslinic Acids derivatives as a promising treatment against bacterial biofilm in nosocomial infections: An in Vitro and in Vivo study.

Núria Blanco-Cabra[1], Karina Vega-Granados[2], Laura Moya-Andérico[1], Marija Vukomanovic[1], Andrés Parra[2], Luis Álvarez de Cienfuegos[2,3*], Eduard Torrents[1,*]

[1]Bacterial infections and antimicrobial therapies group (IBEC), The Barcelona Institute of Science and Technology (BIST) and [2]Department of Organic Chemistry, Faculty of Science, University of Granada. [3]Instituto de Investigación Biosanitaria ibs. Granada. Universidad de Granada. 18012 Granada, Spain.

*Corresponding authors:

Dr. Eduard Torrents: etorrents@ibecbarcelona.eu

Dr. Luis Álvarez de Cienfuegos: lac@ugr.es

Table of Contents

Table S1: Average ± standard deviation and ratio of green and red cells in the Live/Dead analysis.

	CONTROL	OA	MA	MA-HDA-MA	OA-HDA	MA-HDA	MA-DMPA	OA-DAD	MA-DAD
GREEN CELLS (alive)	4450 ± 296.6	15.17 ± 7.3	4 ± 2.8	1570.7 ± 20.8	0.8 ± 1.09	5 ± 2.55	1241 ± 153.9	6.67 ± 4	2.67 ± 3.05
RED CELLS (dead)	76 ± 8.485	68.8 ± 32.16	44.5 ± 14.1	144.33 ± 24.5	34.2 ± 7.12	68.7 ± 18.7	96.25 ± 19.2	31.67 ± 22.85	98 ± 13
RATIO (green/ red)	58.55	0.22	0.09	10.88	0.02	0.07	12.89	0.21	0.03

Table S2: Staphylococcus aureus antimicrobial activity profile.

	Antimicrobial activity profile (MIC_{50} µg/ml)	
Antibiotic	***S. aureus* CECT 86 (ATCC 12600)**	***S. aureus* MRSA**
Linezolid	2	4
Oxacillin	1	>250
Vancomycin	1	1
Daptomycin	0.25	0.5
Ciprofloxacin	0.25	

General Information

To obtain the extract of the raw material, n-Hexane (Merck, ref. 1.04374) and EtOAc (Fisher Scientific, ref. E/0900/17) solvents were used with previous distillation. The isolation of the amino compounds, maslinic and oleanolic acids was carried out by flash chromatography, using silica gel 60 (Merck, ref. 1.09385) as the stationary phase, and CH2Cl2 (Fisher Scientific, ref. D/1852/17), with increasing amounts of Me_2CO (Fisher Scientific, ref. A/0600/17) as the mobile phase. For the control of flash chromatography and reactions, silica gel 60 aluminum sheets (Merk. ref. 1.16835) were used, the compounds were made visible by spraying a mixture of H_2SO_4 and AcOH, followed by heating at 120 °C, and finally observed with UV light at 254 nm. For the amidation reactions were used DIEA (Sigma-Aldrich, ≥99%, ref. D125806), TBTU (Apollo Scientific, ref. PC0921), 3-(Dimethylamino)-1-propylamine (Sigma-Aldrich, ≥98.0%, ref. 39380), 1,3-Diaminopropane (Sigma-Aldrich, ≥98.0%, ref. 239984), 1,6-Diaminohexane (Sigma-Aldrich, 98%, ref. H11696), 1,10-Diaminodecane (ACROS Organics 97%, ref. 112130250), Na_2SO_4 Anhydrous (Fisher Chemical, 99+%, ref. S/6600/65), K_2CO_3 (PanReac AppliChem, ref. 141490), the solvents THF (Sigma-Aldrich, HPLC ≥99%, ref. 270385) with previous distillation, and CH_2Cl_2 (Fisher Scientific, ref. D/1852/17). The reagents were used without further purification. Measurements of NMR spectra were made in VARIAN direct drive (400 and 500 MHz ^1H NMR) spectrometers. The ^{13}C chemical shifts were assigned with the aid of distortion less enhancement by polarization transfer (DEPT) using a flip angle of 135.

MA-PDA

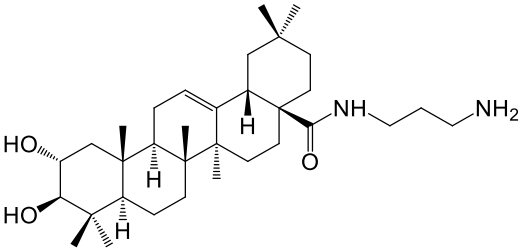

^{1}HNMR($CDCl_3$, 400 MHz): δ 6.43 (dd, 1H, *J*1 = *J*2 = 5.4 Hz), 5.35 (dd, 1H, *J*1 = *J*2 = 3.2 Hz), 3.70 (ddd, 1H, *J*1 = 4.8, *J*2 = 9.6, *J*3 = 14.0 Hz), 3.50–3.41 (m, 1H), 3.13–3.10 (m, 1H), 2.98 (d, 1H, *J* = 9.6 Hz), 2.75 (t, 1H, *J* = 6.4 Hz), 2.52 (dd, 1H, *J*1 = 3.6, *J*2 = 12.8 Hz), 1.15, 1.02, 0.97, 0.90, 0.90, 0.81, 0.75 (s, 3H); ESI-HRMS m/z calculated for $C_{33}H_{57}N_2O_3$ $[M+1]^+$ 529.4369, found 529.4336.

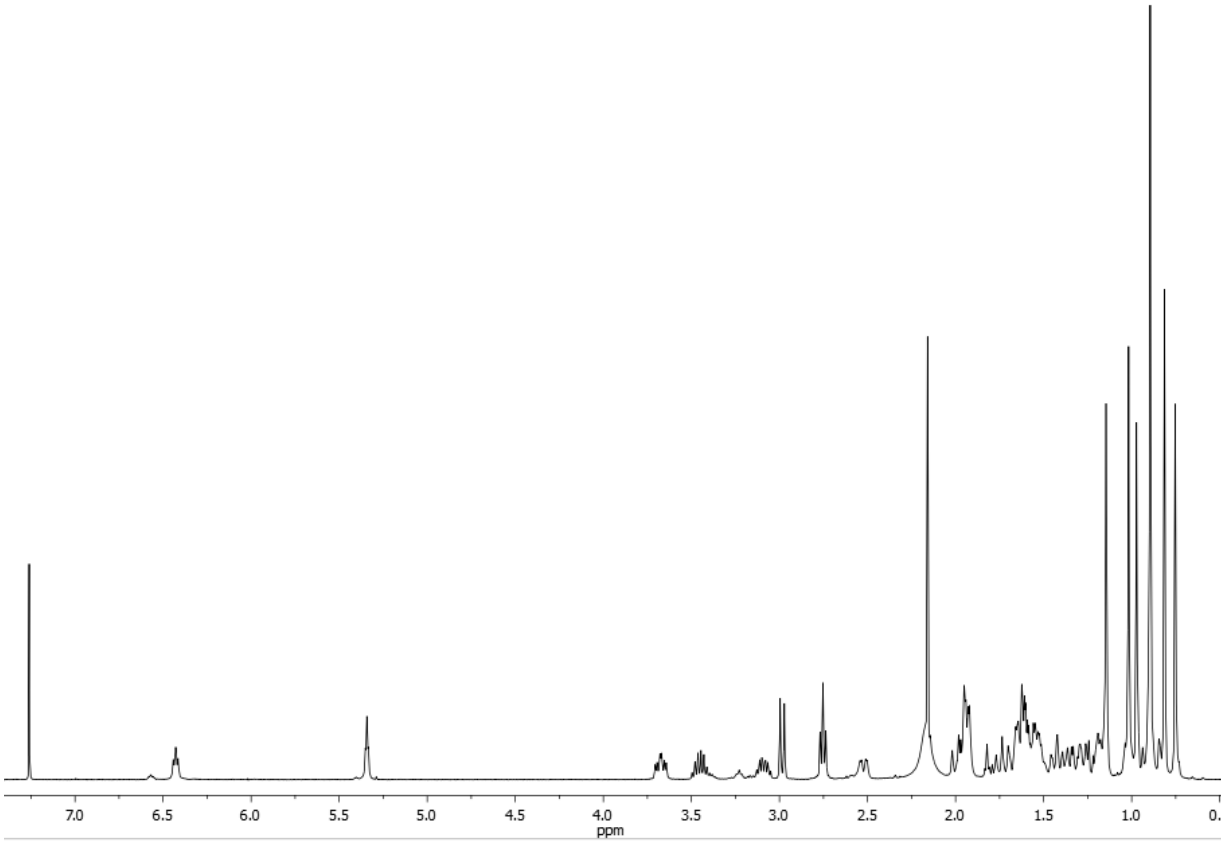

OA-PDA

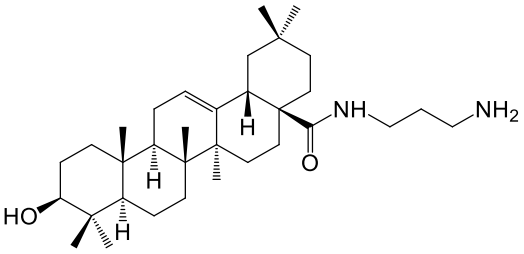

^{1}HNMR($CDCl_3$, 400 MHz): δ 6.41 (dd, 1H, *J*1 = *J*2 = 5.0 Hz), 5.35 (dd, 1H, *J*1 = *J*2 = 3.2 Hz), 3.49–3.44 (m, 1H), 3.21 (dd, 1H, *J*1 = 4.6, *J*2 = 8.8 Hz), 3.13–3.10 (m, 1H), 2.77 (t, 2H, *J* = 6.0 Hz), 2.52 (dd, 1H, *J*1 = 3.4, *J*2 = 13.0 Hz), 1.25, 1.15, 0.98, 0.90, 0.90, 0.78, 0.76 (s, 3H); ESI-HRMS m/z calculated for $C_{33}H_{57}N_2O_2$ $[M+1]^+$ 513.4420, found 513.4426.

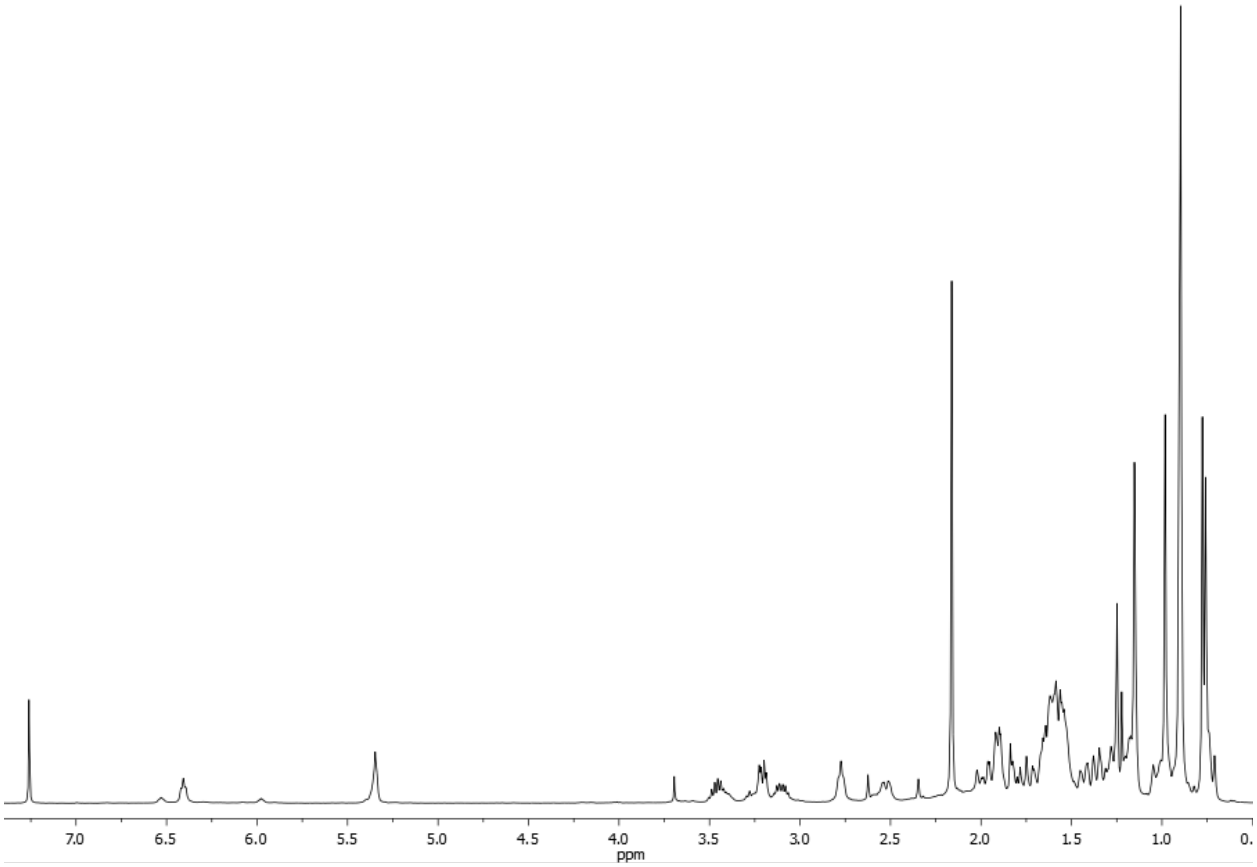

MA-HDA

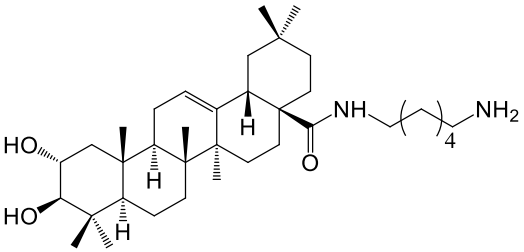

^{1}HNMR($CDCl_3$, 400 MHz): δ 5.90 (dd, 1H, *J*1 = *J*2 = 5.4 Hz), 5.36 (dd, 1H, *J*1 = *J*2 = 3.2 Hz), 3.68 (ddd, 1H, *J*1= 4.8, *J*2 = 9.2, *J*3 = 14.0 Hz), 3.35–3.32 (m, 1H), 3.19–3.15 (m, 1H), 2.98 (d, 1H, *J* = 9.2 Hz), 2.69 (t, 2H, *J* = 6.4 Hz), 2.49 (dd, 1H, *J*1 = 3.6, *J*2 = 12.8 Hz), 1.15, 1.02, 0.98, 0.90, 0.90, 0.82, 0.75 (s, 3H); ESI-HRMS m/z calculated for $C_{36}H_{63}N_2O_3$ $[M+1]^+$ 571.4839, found 571.4842.

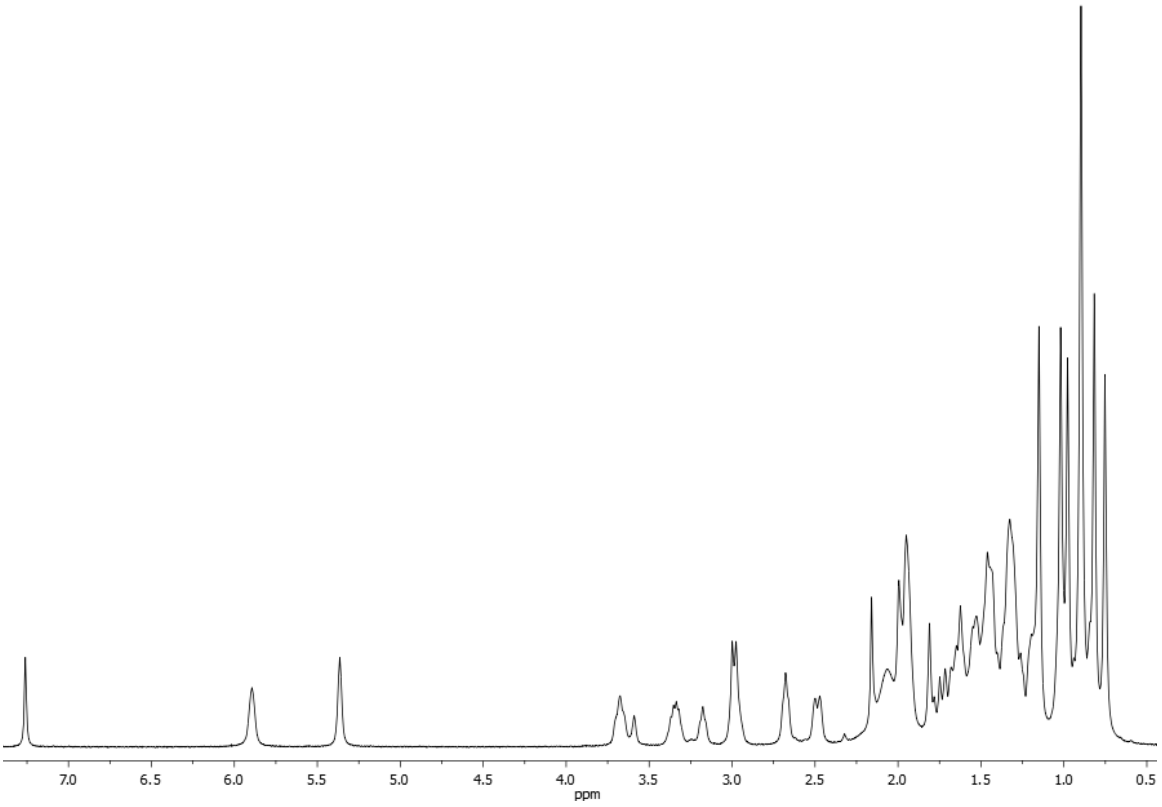

OA-HDA

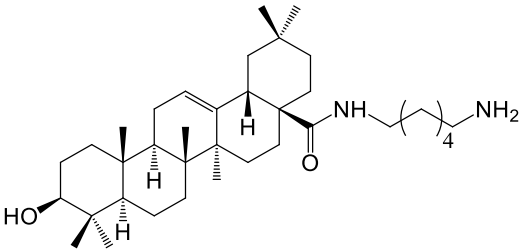

^{1}HNMR($CDCl_3$, 400 MHz): δ 5.96 (dd, 1H, *J*1 = *J*2 = 6.0 Hz), 5.37 (dd, 1H, *J*1 = *J*2 = 2.8 Hz), 3.37–3.32 (m, 1H), 3.21 (dd, 1H, *J*1 = 4.4, *J*2 = 10.8 Hz), 2.98–2.94 (m, 1H), 2.78 (t, 2H, *J* = 6.0 Hz), 2.50 (dd, 1H, *J*1 = 2.8, *J*2 = 13.2 Hz), 1.15, 0.98, 0.91, 0.90, 0.90, 0.78, 0.75 (s, 3H); ESI-HRMS m/z calculated for $C_{36}H_{63}N_2O_2$ $[M+1]^+$ 555.4890, found 555.4874.

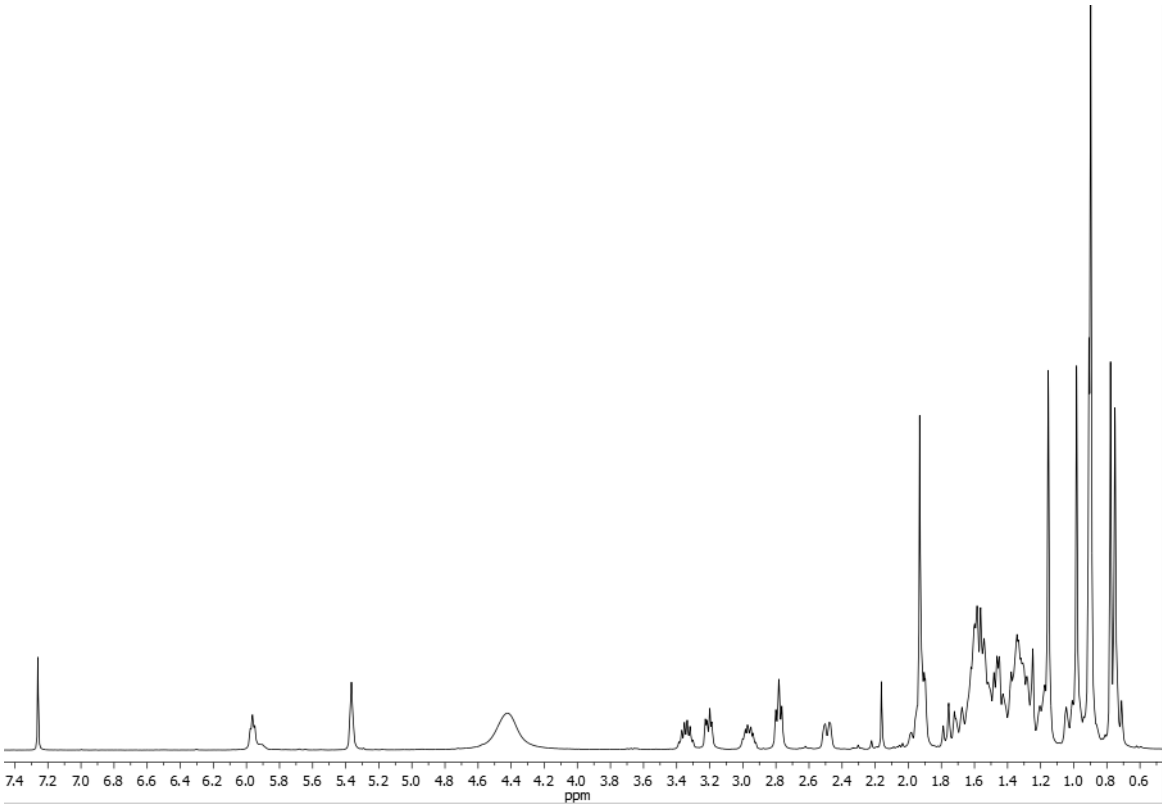

MA-DAD

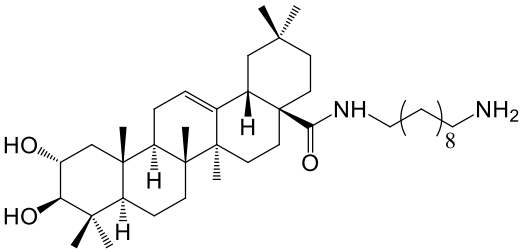

^{1}HNMR($CDCl_3$, 400 MHz): δ 5.91 (dd, 1H, *J*1 = *J*2 = 4.8 Hz), 5.36 (dd, 1H, *J*1 = *J*2 = 2.8 Hz), 3.68 (ddd, 1H, *J*1= 4.0, *J*2 = 9.6, *J*3 = 14.0 Hz), 3.36–3.28 (m, 1H), 3.06–2.99 (m, 1H), 3.00 (d, 1H, *J* = 9.6 Hz), 2.68 (t, 2H, *J* = 6.4 Hz), 2.50 (dd, 1H, *J*1 = 2.4, *J*2 = 12.4 Hz), 1.28, 1.16, 1.03, 0.99, 0.90, 0.82, 0.76 (s, 3H); ESI-HRMS m/z calculated for $C_{40}H_{71}N_2O_3$ $[M+1]^+$ 627.5386, found 627.5478.

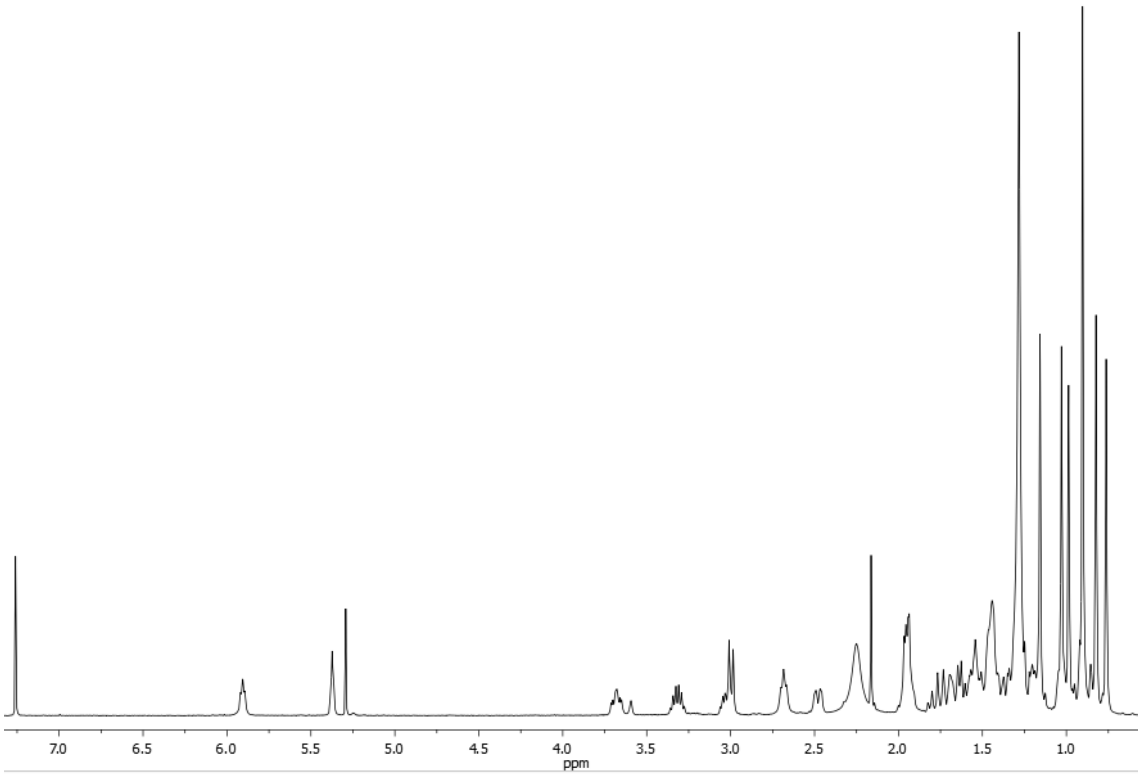

OA-DAD

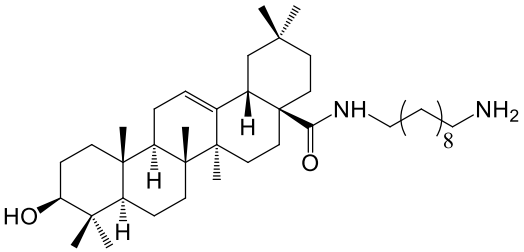

^{1}HNMR($CDCl_3$, 400 MHz): δ 6.41 (dd, 1H, *J*1 = *J*2 = 5.2 Hz), 5.35 (dd, 1H, *J*1 = *J*2 = 3.2 Hz), 3.49–3.39 (m, 1H), 3.21 (dd, 1H, *J*1 = 4.6, *J*2 = 11.1 Hz), 3.14–3.07 (m, 1H), 2.77 (t, 2H, *J* = 6.0 Hz), 2.52 (dd, 1H, *J*1 = 3.6, *J*2 = 13.2 Hz), 1.25, 1.15, 0.98, 0.91, 0.90, 0.78, 0.76 (s, 3H); ESI-HRMS m/z calculated for $C_{40}H_{71}N_2O_2$ $[M+1]^+$ 611.5516, found 611.5534.

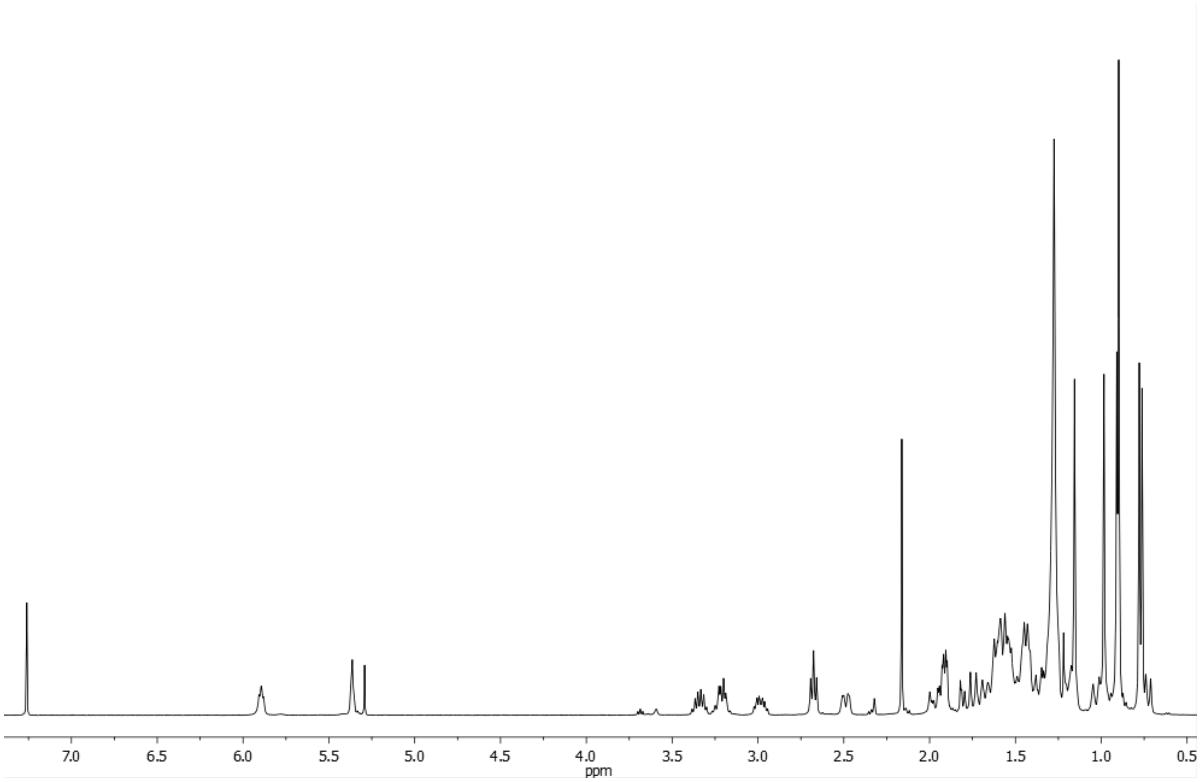

MA-DMPA

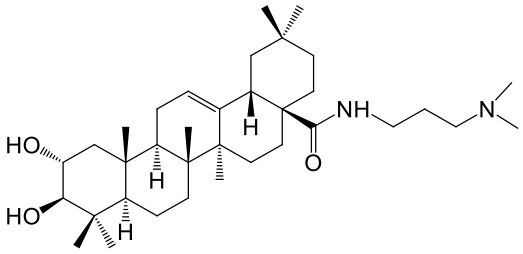

^{1}HNMR($CDCl_3$, 500 MHz): δ 7.01 (dd, 1H, *J*1 = *J*2 = 5.4 Hz), 5.30 (dd, 1H, *J*1 = *J*2 = 3.6 Hz), 3.66 (ddd, 1H, *J*1 = 4.8, *J*2 = 9.6, *J*3 = 14.0 Hz), 3.53–3.45 (m, 1H), 3.00–2.98 (m, 1H), 2.97 (d, 1H, *J* = 9.5 Hz), 2.51 (dd, 1H, *J*1 = 3.6, *J*2 = 12.8 Hz), 2.25, 2.25, 1.12, 1.01, 0.95, 0.89, 0.88, 0.80 0.73 (s, 3H). ^{13}CNMR ($CDCl_3$, 126 MHz): δ 178.10 (C), 144.80 (C), 122.53 (CH), 83.92 (CH), 68.90 (CH), 58.81(CH_2), 55.34(CH), 53.95(CH_2), 47.68(CH), 46.88 (CH_2), 46.44 (CH_2), 46.22 (C), 45.62 (CH), 42.04 (C), 41.99 (CH_3), 39.54 (C), 39.30 (CH_2), 38.32 (C), 34.24 (CH_2), 33.16 (CH_3), 32.99 (CH_2), 32.39 (CH_2), 31.86 (C), 30.84 (C), 29.39 (CH_3), 28.75 (CH_3), 27.44 (CH_2), 26.07 (CH_3), 26.05 (CH_2), 23.67 (CH_3), 23.63(CH_2), 18.44 (CH_2), 17.04 (CH_3), 16.90 (CH_3), 16.73 (CH_3). ESI-HRMS m/z calculated for $C_{35}H_{61}N_2O_3$ $[M+1]^+$ 557.4604, found 557.4682.

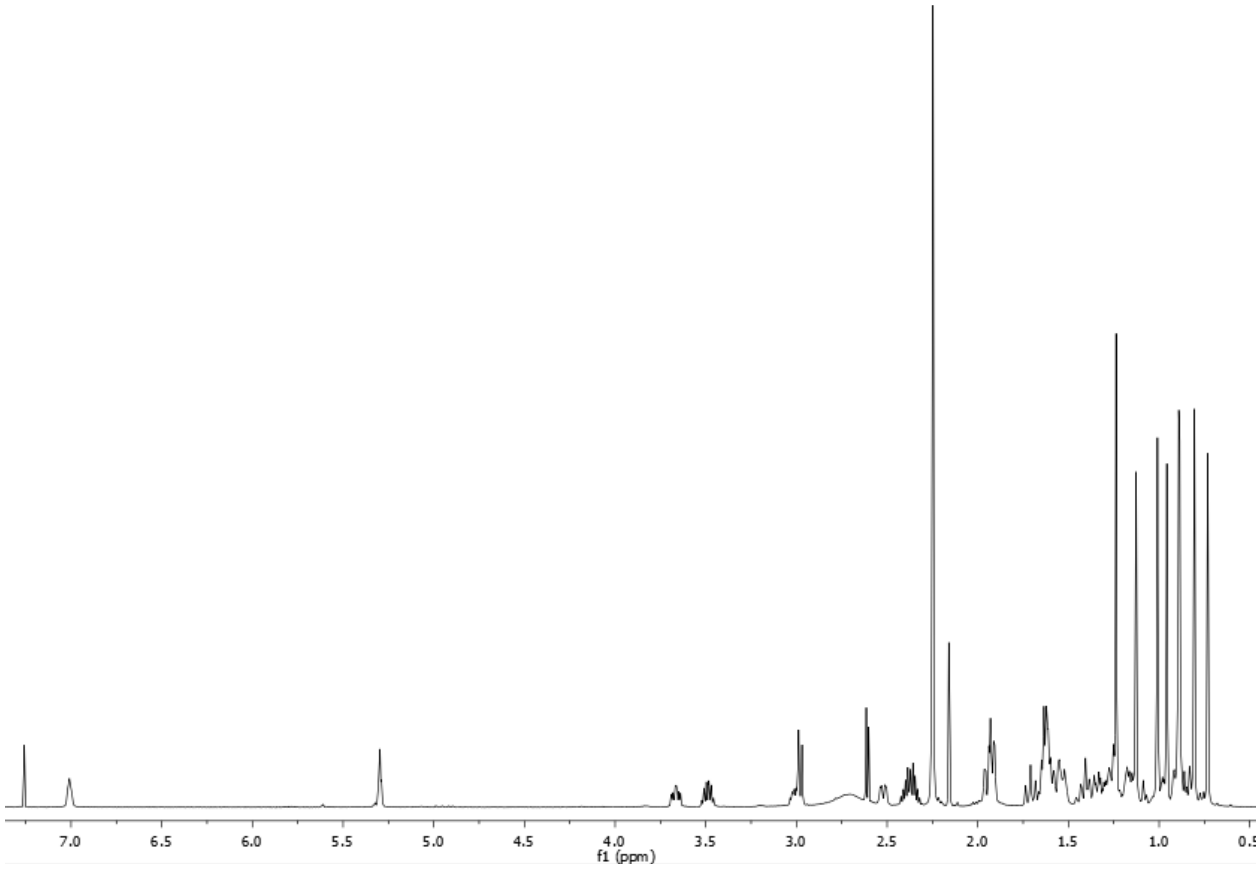

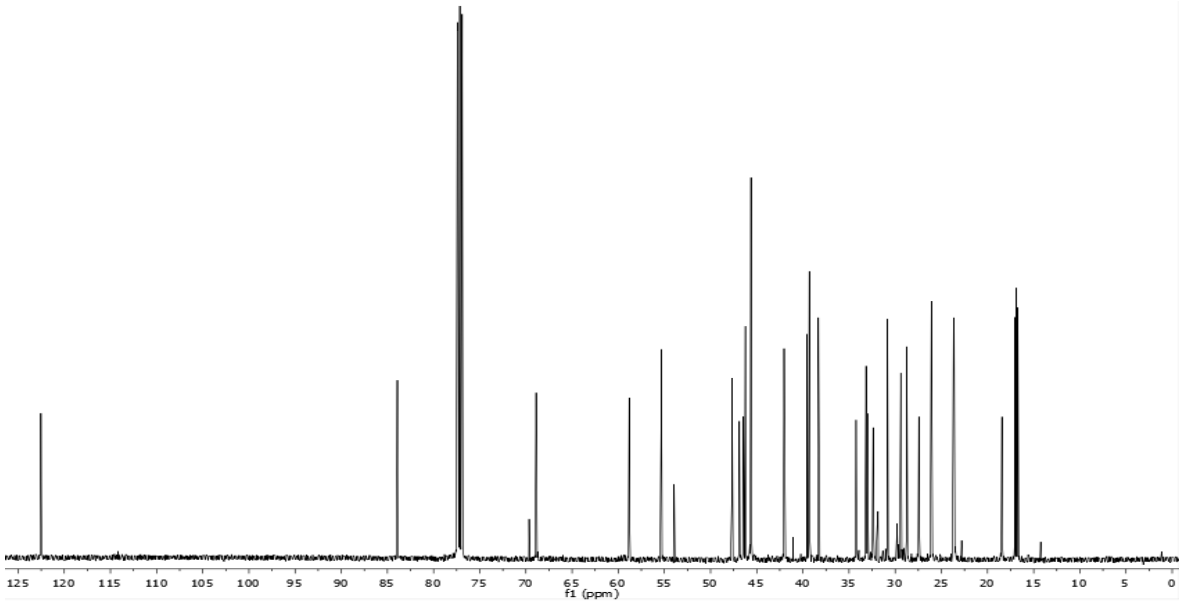
125 120 115 110 105 100 95 90 85 80 75 70 65 60 55 50 45 40 35 30 25 20 15 10 5 0
f1 (ppm)

OA-DMPA

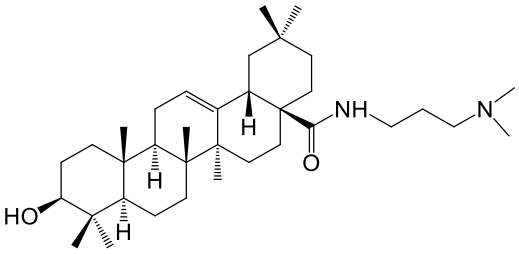

^{1}HNMR($CDCl_3$, 500 MHz): δ 6.78 (dd, 1H, *J*1 = *J*2 = 5.3 Hz), 5.34 (dd, 1H, *J*1 = *J*2 = 3.7 Hz), 3.47–3.40 (m, 1H), 3.18 (dd, 1H, *J*1 = 4.6, *J*2 = 11 Hz), 3.09–3.02 (m, 1H), 2.58 (dd, 1H, *J*1 = 3.4, *J*2 = 13.0 Hz), 2.37, 2.37, 1.13, 0.97, 0.90, 0.89, 0.89, 0.77, 0.73 (s, 3H). ^{13}CNMR ($CDCl_3$, 126 MHz): δ 178.44 (C), 144.80 (C), 122.75 (CH), 79.09 (CH), 57.17 (CH_2), 55.28 (CH), 47.71 (CH), 46.85(CH_2), 46.34 (C), 44.43 (CH), 42.04 (C), 41.95 (CH_3), 39.51(C), 38.89 (C), 38.57 (CH_2), 38.17 (CH_2), 37.13 (C), 34.28 (CH_2), 33.18 (CH_3), 33.03 (CH_2), 32.54 (CH_2), 30.86 (C), 28.23(CH_3), 27.50 (CH_2), 27.29 (CH_2), 26.03 (CH_3), 25.69 (CH_2), 23.73 (CH_3), 23.64 (CH_2), 23.60 (CH_2), 22.68 (CH_3), 18.44 (CH_2), 17.07 (CH_3), 15.71 (CH_3), 15.46 (CH_3).ESI-HRMS m/z calculated for $C_{35}H_{61}N_2O_2$ $[M+1]^+$ 541.4655, found 541.4733.

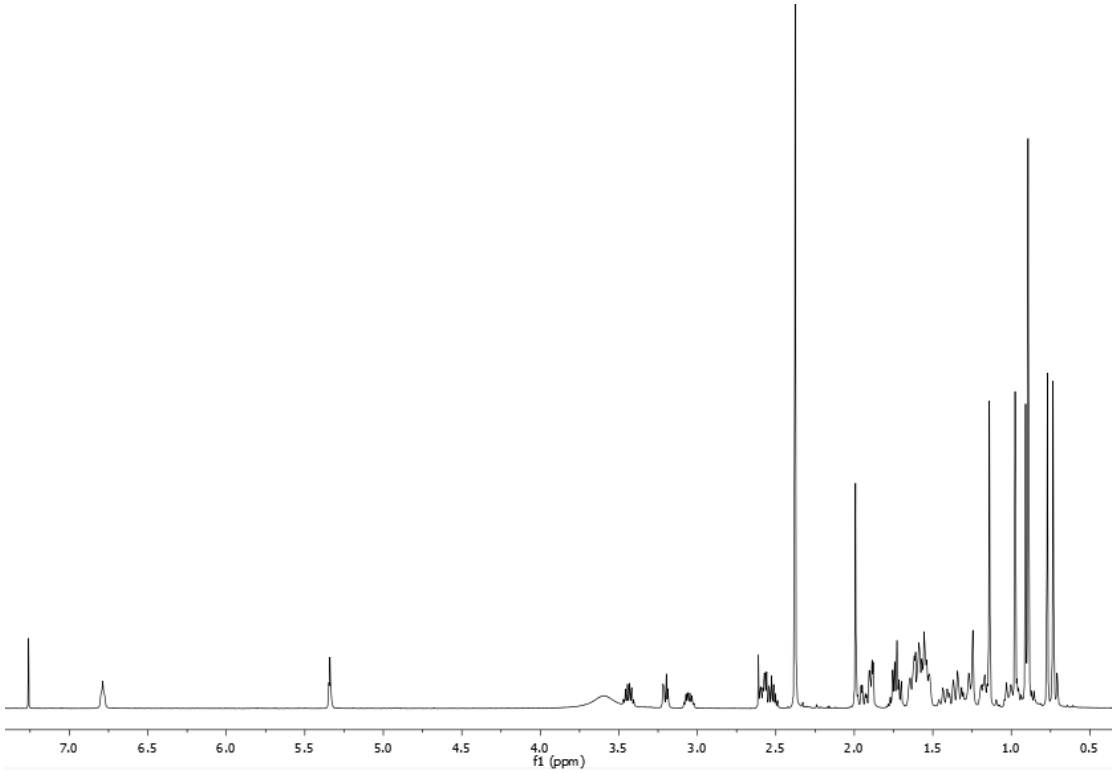

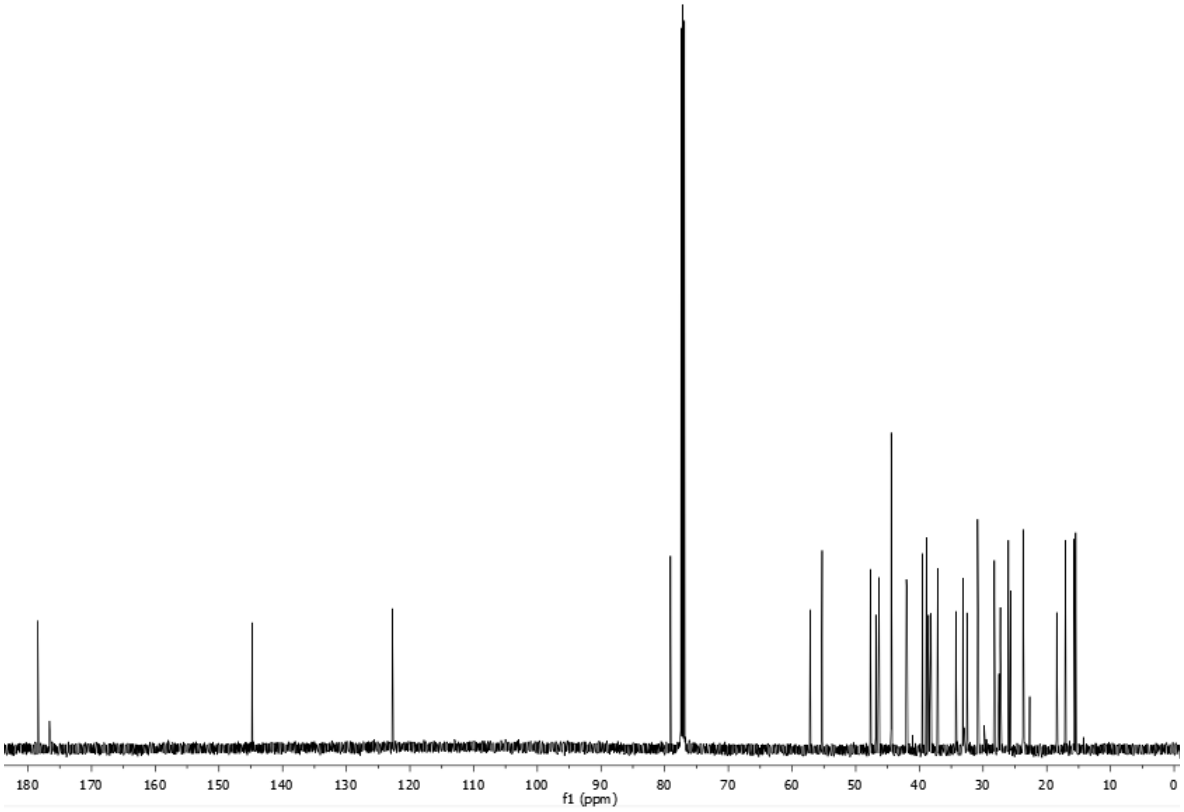
180
170
160
150
140
130
120
110
100
90
80
70
60
50
40
30
20
10
0
f1 (ppm)

MA-PDA-MA

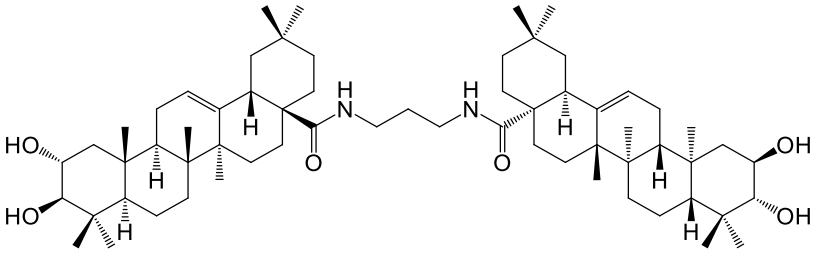

^{1}HNMR($CDCl_3$, 400 MHz): δ 6.43 (dd, 1H, *J*1 = *J*2 = 6.0 Hz), 5.35 (dd, 1H, *J*1 = *J*2 = 3.2 Hz), 3.70 (ddd, 1H, *J*1 = 4.0, *J*2 = 9.2, *J*3 = 14.0 Hz), 3.28–3.23 (m, 1H), 3.15–3.10 (m, 1H), 3.01 (d, 1H, *J* = 9.2 Hz), 2.65 (dd, 1H, *J*1 = 3.6, *J*2 = 13.2 Hz), 1.16, 1.03, 0.98, 0.92, 0.91, 0.83, 0.74 (s, 3H); ESI-HRMS m/z calculated for $C_{63}H_{103}N_2O_6$ $[M+1]^+$ 983.7816, found 983.7781.

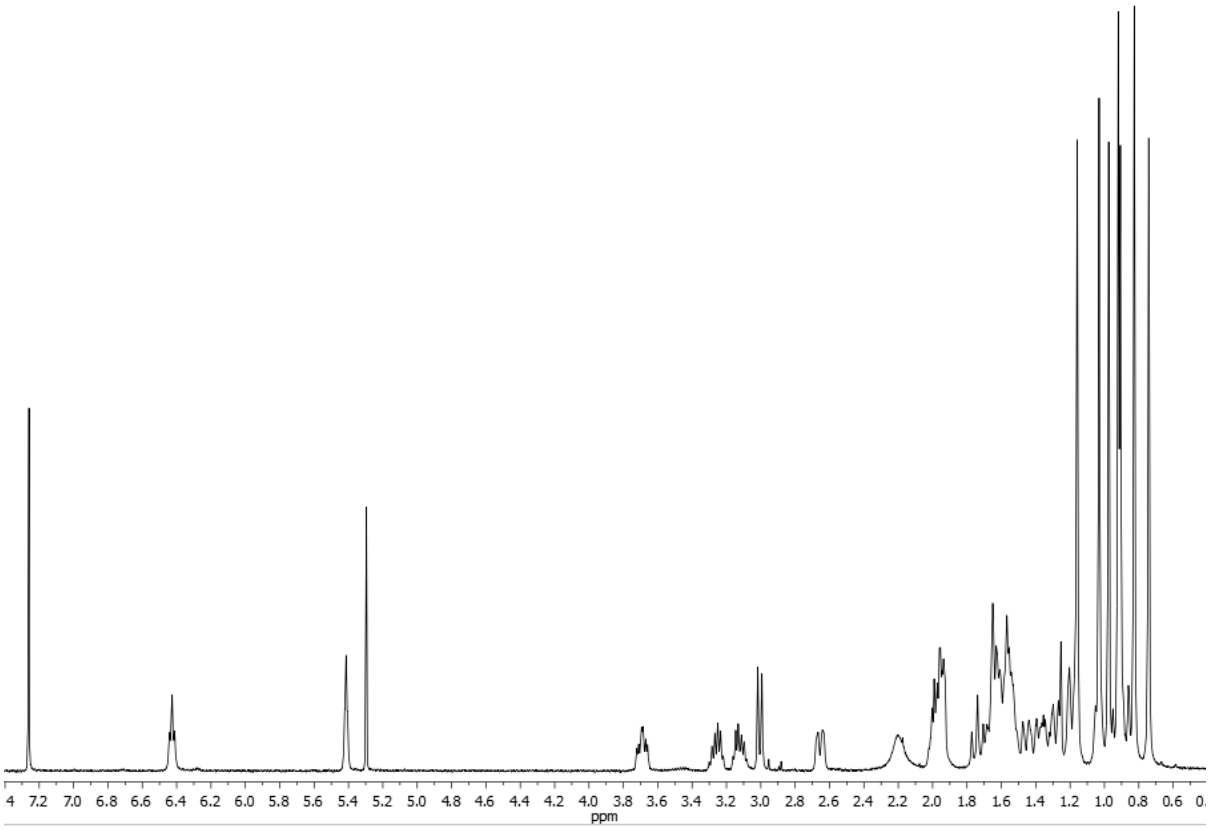

OA-PDA-OA

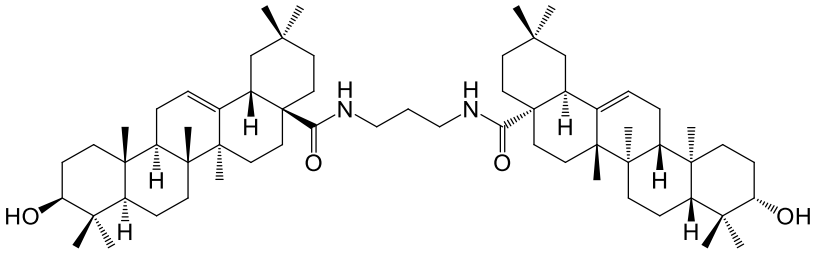

^{1}HNMR($CDCl_3$, 400 MHz): δ 6.41 (dd, 1H, *J*1 = *J*2 = 6.0 Hz), 5.40 (dd, 1H, *J*1 = *J*2 = 3.2 Hz), 3.28–3.24 (m, 1H), 3.21 (dd, 1H, *J*1 = 4.8, *J*2 = 11.21 Hz), 3.14–3.10 (m, 1H), 2.64 (dd, 1H, *J*1 = 3.2, *J*2 = 14.4 Hz), 1.25, 1.15, 0.98, 0.91, 0.90, 0.77, 0.74 (s, 3H); ESI-HRMS m/z calculated for $C_{63}H_{101}N_2O_4$ $[M+1]^+$ 949.7761, found 949.7772.

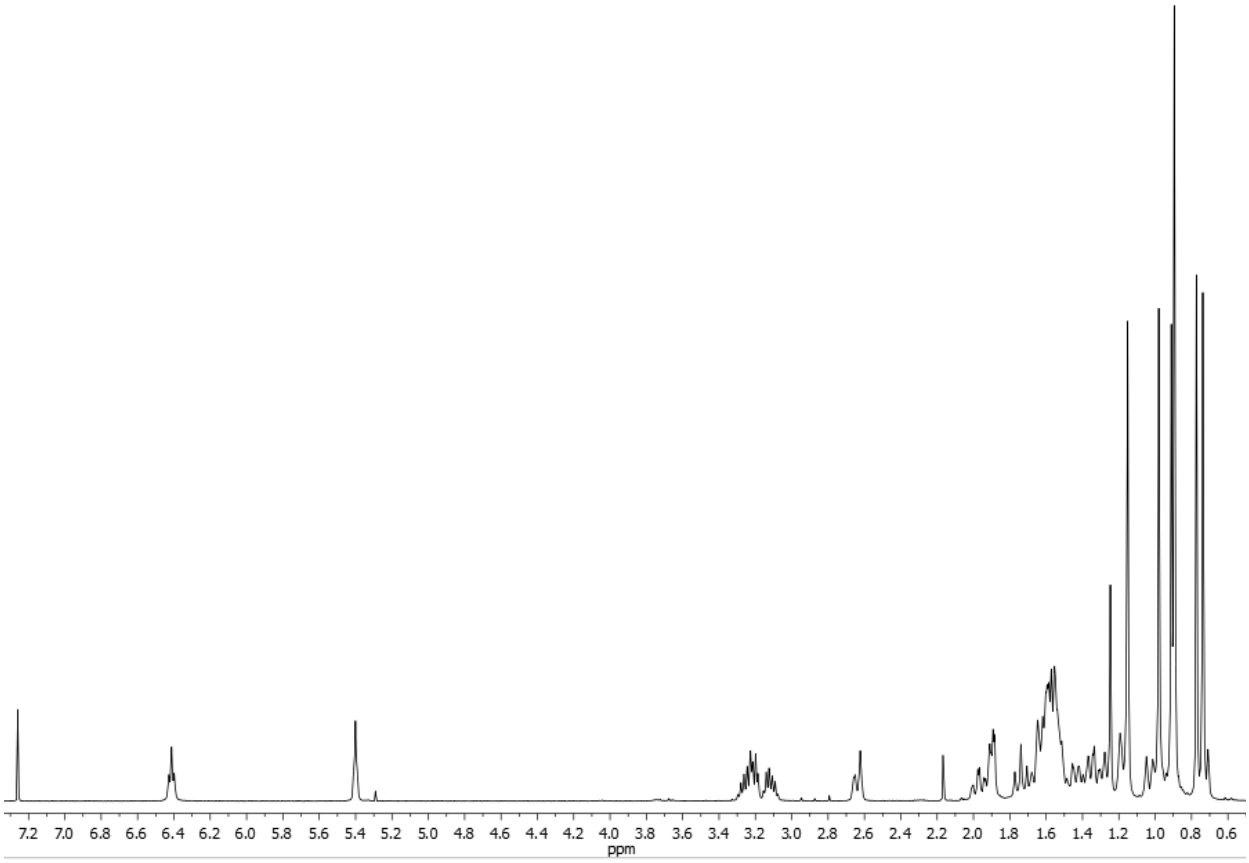

MA-HDA-MA

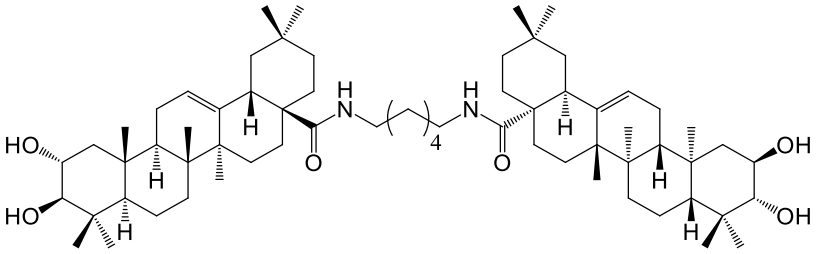

^{1}HNMR(CDCl3, 400 MHz): δ 5.94 (dd, 1H, *J*1 = *J*2 = 5.4 Hz), 5.38 (dd, 1H, *J*1 = *J*2 = 3.2 Hz), 3.70 (ddd, 1H, *J*1 = 4.4, *J*2 = 9.2, *J*3 = 13.6 Hz), 3.38–3.30 (m, 1H), 3.01–2.94 (m, 1H), 3.00 (d, 1H, *J* = 9.2 Hz), 2.50 (dd, 1H, *J*1 = 3.2, *J*2 = 12.8 Hz), 1.25, 1.16, 1.03, 0.99, 0.90, 0.83, 0.76 (s, 3H); ESI-HRMS m/z calculated for $C_{66}H_{109}N_2O_6$ $[M+1]^+$ 1025.8286, found 1025.8268.

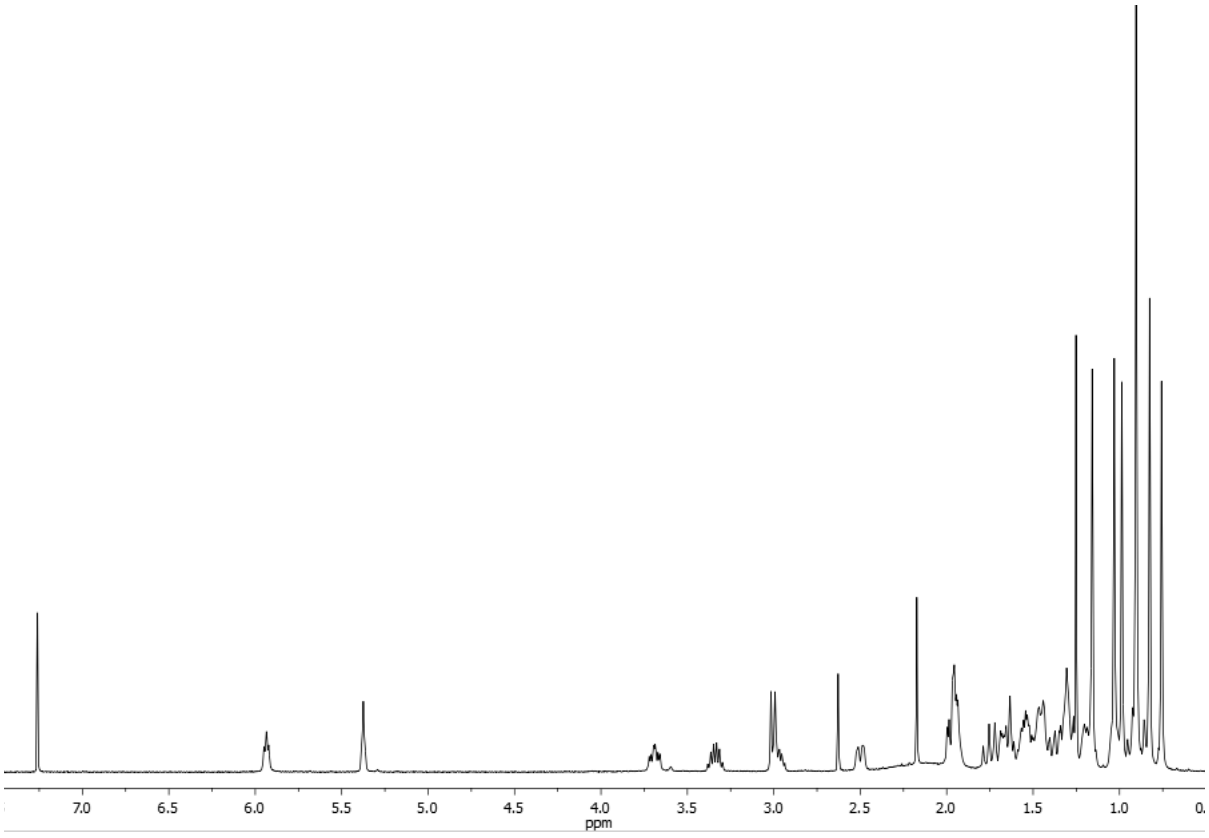

OA-HDA-OA

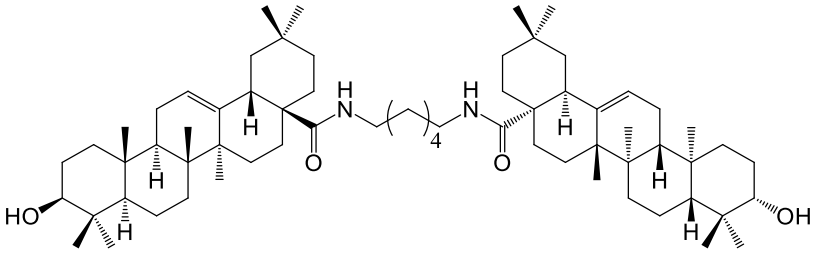

^{1}HNMR($CDCl_3$, 400 MHz): δ 5.95 (dd, 1H, *J*1 = *J*2 = 5.2 Hz), 5.36 (dd, 1H, *J*1 = *J*2 = 3.0 Hz), 3.35–3.30 (m, 1H), 3.20 (dd, 1H, *J*1 =4.2, *J*2 = 11.0 Hz), 3.00–2.93 (m, 1H), 2.48 (dd, 1H, *J*1 = 3.2, *J*2 = 13.2 Hz),1.14, 0.97, 0.89, 0.89, 0.88, 0.77, 0.74 (s, 3H); ESI-HRMS m/z calculated for $C_{66}H_{107}N_2O_4$ $[M+1]^+$ 991.8231, found 991.8235.

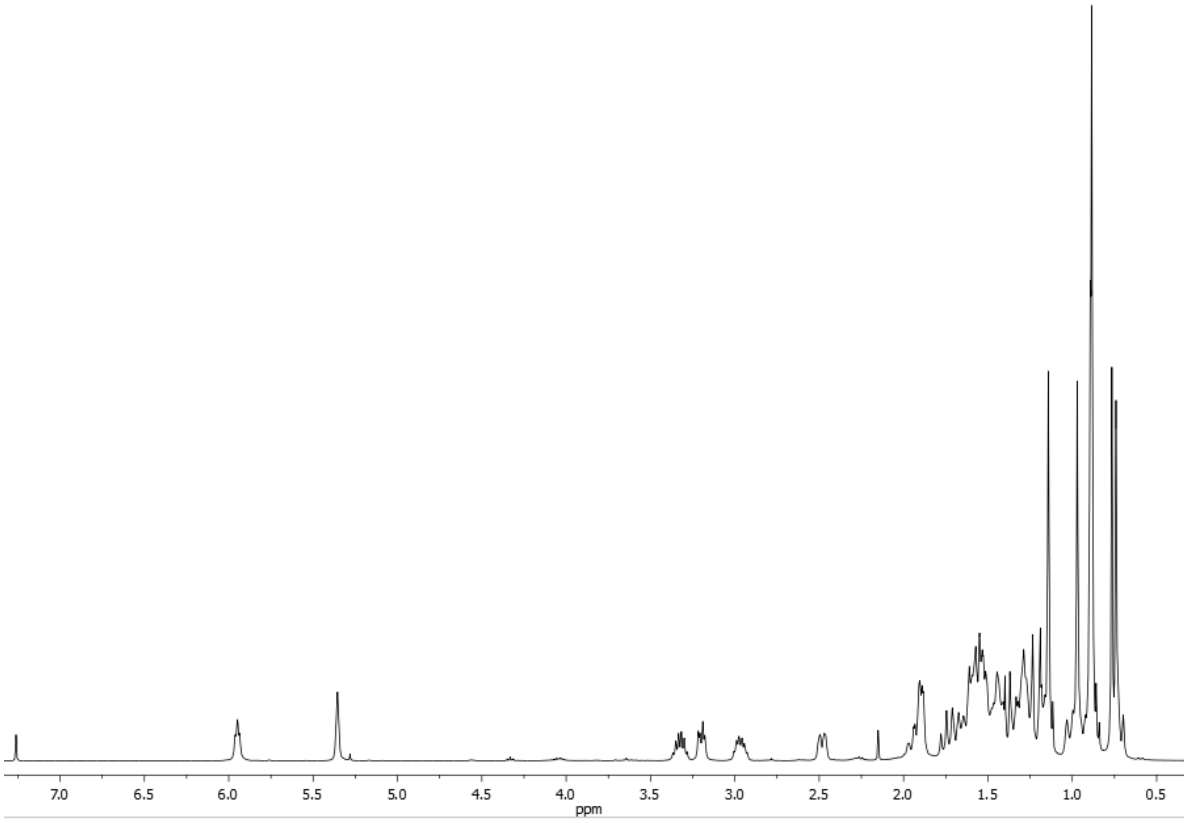

MA-DAD-MA

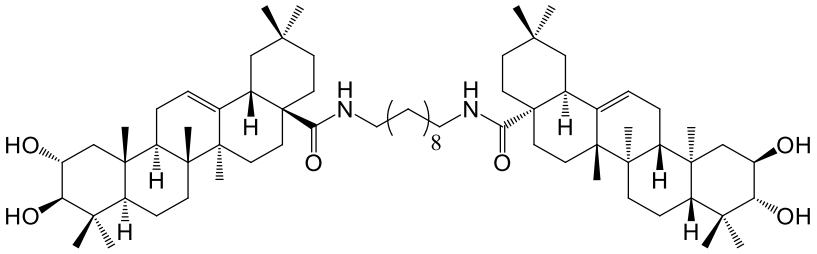

^{1}HNMR(CDCl3, 400 MHz): δ 5.94 (dd, 1H, *J*1 = *J*2 = 5.2 Hz), 5.37 (dd, 1H, *J*1 = *J*2 = 3.2 Hz), 3.69 (ddd, 1H, *J*1 = 4.4, *J*2 = 9.6, *J*3 = 14 Hz), 3.35–3.29 (m, 1H), 3.02–2.96 (m, 1H), 3.51 (d, 1H, *J* = 9.6 Hz), 2.47 (dd, 1H, *J*1 = 3.2, *J*2 = 12.4 Hz), 1.25, 1.16, 1.03, 0.98, 0.90, 0.83, 0.76 (s, 3H); ESI-HRMS m/z calculated for $C_{70}H_{117}N_2O_6$ $[M+1]^+$ 1081.8912, found 1081.8900.

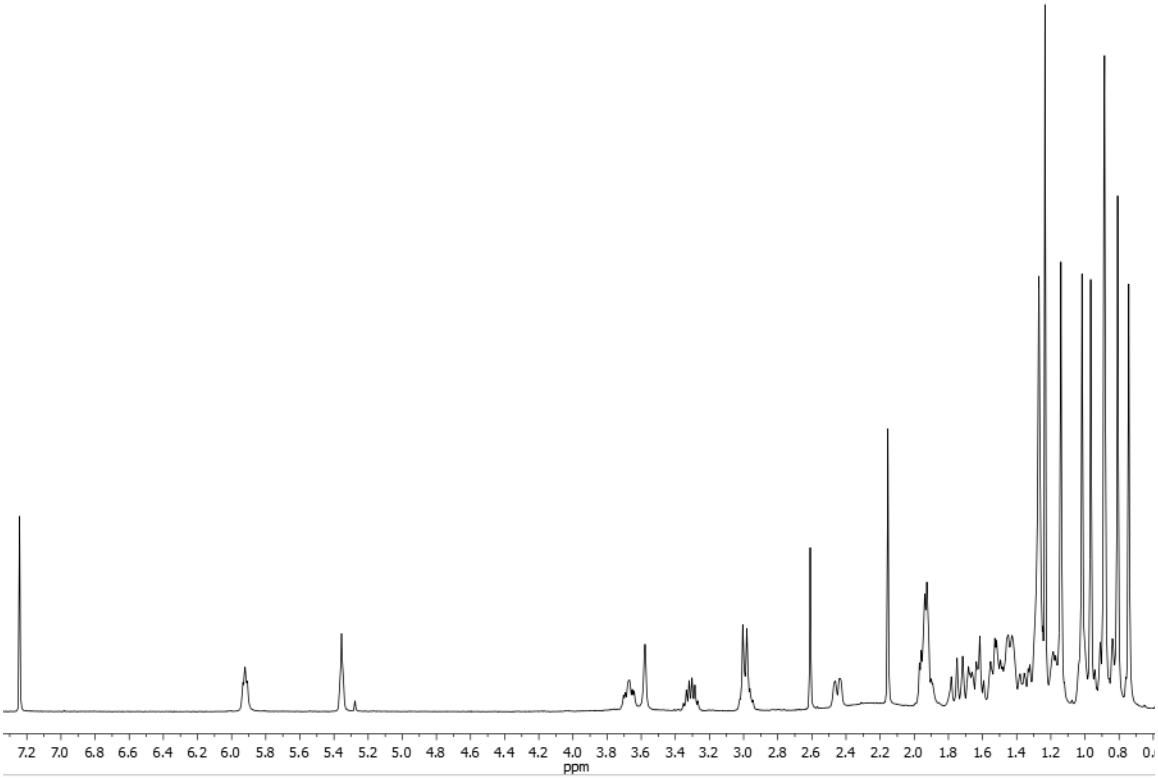

OA-DAD-OA

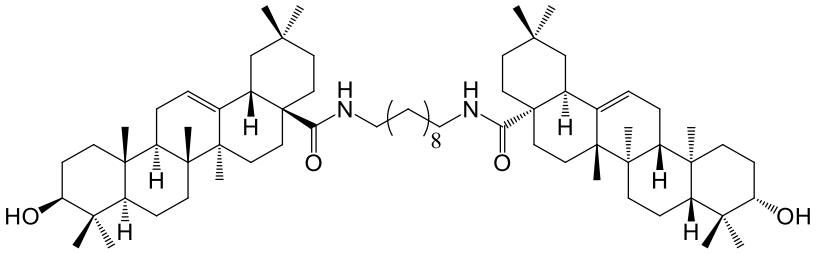

^{1}HNMR($CDCl_3$, 400 MHz): δ 5.90 (dd, 1H, *J*1 = *J*2 = 4.8 Hz), 5.36 (dd, 1H, *J*1 = *J*2 = 2.8 Hz), 3.37–3.32 (m, 1H), 3.21 (dd, 1H, *J*1 =4.4, *J*2 = 10.8 Hz), 3.00–2.93 (m, 1H), 2.49 (dd, 1H, *J*1 = 2.6, *J*2 = 12.6 Hz),1.25, 1.15, 0.98, 0.91, 0.90, 0.78, 0.76 (s, 3H); ESI-HRMS m/z calculated for $C_{70}H_{117}N_2O_4$ $[M+1]^+$ 1049.9013, found 1049.8990.